PERIODICO di MINERALOGIA
established in 1930

DIPARTIMENTO
DI SCIENZE DELLA TERRA

SAPIENZA
UNIVERSITÀ DI ROMA

An International Journal of
Mineralogy, Crystallography, Geochemistry,
Ore Deposits, Petrology, Volcanology
and applied topics on Environment, Archaeometry and Cultural Heritage

Secondary mineral assemblages as indicators of multistage alteration processes in basaltic lava flows: evidence from the Lessini Mountains, Veneto Volcanic Province, Northern Italy

Michele Mattioli [a,*], Marco Cenni [a], Elio Passaglia [b]

[a] Dipartimento di Scienze della Terra, della Vita e dell'Ambiente, Università di Urbino "Carlo Bo", Urbino, Italy
[b] Dipartimento di Scienze Chimiche e Geologiche, Università di Modena e Reggio Emilia, Italy

ARTICLE INFO

Submitted: October2014
Accepted: July 2015
Available on line: November 2015

* Corresponding author:
michele.mattioli@uniurb.it

DOI: 10.2451/2015PM0375

How to cite this article:
Mattioli M. et al. (2016) Period. Mineral. 85, 1-24

ABSTRACT

The secondary mineral assemblages in the Tertiary basalts from the Lessini Mountains are mainly clay minerals and zeolites, and result from multistage alteration processes. In the earliest Stage I, clay and silica minerals precipitate along the inner walls of the vesicles, followed by the deposition of the fine-grained zeolites of the Stage II (erionite, offretite, analcime, natrolite, heulandite and stilbite). The final Stage III is marked by a new generation of large, well-shaped zeolites (phillipstite-harmotomo, gmelinite, chabazite, willhendersonite and yugawaralite), followed by extensive crystallization of calcite. New morphological and chemical data are presented herein in order to reveal the chemical compositions of Lessini zeolite species, which have never been analyzed before. Textural and chemical observations indicate that the chemical elements for Stage I and II alteration minerals derived from the alteration of the basaltic glass and the primary phases in the volcanic host rocks. The final mineral assemblages of the Stage III suggest a variation in the crystallization conditions, probably related to the presence of new, late-stage fluids enriched in Ca and $(CO_3)^{2-}$, leached from the surrounding calcareous rocks.

Keywords: Lessini; Basaltic rocks; Hydrothermal alteration; Secondary minerals; Zeolites.

INTRODUCTION

The secondary mineral assemblages of basaltic rocks, often characterized by clay minerals and zeolites, are useful indicators of the thermal history of volcanic provinces and alteration processes (e.g. Robert et al., 1988; Wise and Kleck, 1988; Schenato et al., 2003; Weisenberger and Bucher, 2011; Weisenberger et al., 2014). Detailed textural (i.e. cross-cutting relationships), mineralogical and geochemical investigations on a small scale can provide helpful information about the thermal evolution of basaltic rock piles (Neuhoff et al., 1999; Franzson et al., 2008; Kousehlar et al., 2012), whereas a careful study of mineral assembles of individual stage can give information about the fluid evolution with time (Robert, 2001; Graham et al., 2003; Weisenberger and Selbekk, 2008).

Secondary minerals in the amygdales, vugs and veins of basaltic lava flows are commonly considered the result of hydrothermal alteration events (Mas et al., 2006; Markússon and Stefánsson, 2011) or low-grade metamorphic reactions during the burial stage (Walker, 1960a; 1960b; Neuhoff et al., 1999; Weisenberger and Selbekk, 2008). In particular, clay minerals in basalt alteration systems are believed to have formed from the interaction of residual fluids during immediate post-eruptive cooling with primary phases and mesostasis glass (Degraff et al., 1989; McMillan et al., 1987; Marescotti et al., 2000; Schenato et al., 2003). The crystallization of zeolites in the vugs of basalt was sometimes thought to result from reactions of the glass with meteoric waters slowly percolating in the rock-fractures at surface temperature (Nashar and Davies, 1960; Nashar and Basden, 1965). Alternatively, it was assumed that they formed via an interaction of volcanic glass (or detrital clays) with saline alkaline lake water (Hay, 1970; Mees et al., 2005). Alteration processes of basaltic rocks involves several

processes such as dissolution of primary phases, deposition of authigenic minerals, ionic exchange and sorption. These processes are mainly dependent on (i) the chemistry and mineralogy of the rocks, and (ii) the chemical features of the interacting fluids (Robert et al., 1988; Franzson et al., 2008; Weisenberger and Bucher, 2011; Gysi and Stefansson, 2012; Kousehlar et al., 2012).

The Tertiary basalts of the Lessini Mountains (Veneto Volcanic Province, Northern Italy) are known to be suitable host rocks for the development of secondary mineral associations (Mattioli et al., 2008; Cenni, 2009). Some zeolites such as gmelinite, analcime, chabazite and phillipsite have already been observed in vesicles of the basaltic rock of Monte Calvarina (Galli, 1972), whereas offretite, chabazite, phillipsite, harmotome, analcime and smectite were discovered in the vugs of volcanites outcropping near Fittà (Passaglia et al., 1996). However, integrated regional studies of the Lessini basalt alteration have yet to be undertaken, and none of the previous studies describe the habits, compositions, mineral associations and paragenetic sequences of the full secondary mineralization in these rocks.

In this paper we present a detailed characterization of the mineralogy, chemical composition, and occurrence of secondary mineral assemblages (mainly zeolite and mafic phyllosilicate) developed within vesicles and veins in the basaltic rocks of the Lessini Mountains. The objectives of this investigation are: 1) to establish the origin and paragenetic sequence of the zeolites and mafic phyllosilicates in this area, and 2) to discuss the geochemical evolution of the basalt system that may possibly account for the pattern of alteration observed. Descriptions and paragenetic sequences are based on a larger sample set (more than 300 samples), although the analyses were conducted on a set of selected samples. We also report here a comparative geochemical study between the fresh (or less-altered) host rocks and their altered equivalents, coming from the same lava flows.

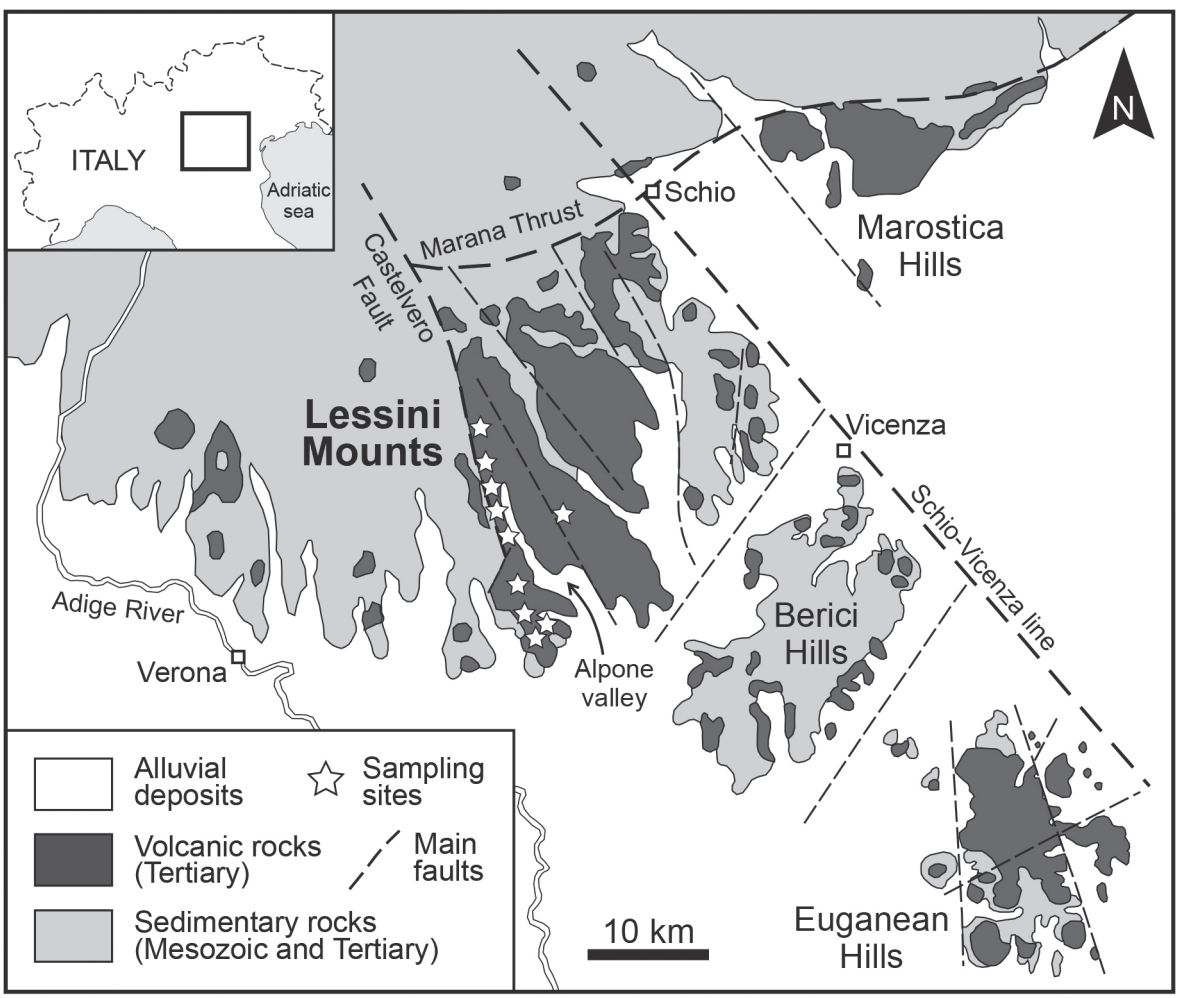

Figure 1. Simplified geological map of the Veneto Volcanic Province (modified from De Vecchi and Sedea, 1995) showing the Lessini Mountains and location of the studied samples.

Although the study of these samples can not be considered as representative for all rock units present at the Lessini Mountains, it is pertinent to note that such a methodology (study of a single lava flow having both "fresh" and "altered" parts) has been highly successful to study the mineralogical and chemical effects of low-temperature alteration in oceanic basalts (Verma, 1981; 1992).

GEOLOGICAL SETTING

The Veneto Volcanic Province is located in Northern Italy and extends over an area of about 2000 km^2 (Figure 1). Due to its tensional tectonic setting, which developed in the South Alpine foreland (Zampieri, 1995; 2000), extensive volcanic activity occurred from the Tertiary, with the greatest part of the eruptions taking place in submarine environments. Several magmatic pulses occurred between the Late Paleocene and the Miocene, all of which were of a short duration and separated by periods of magmatic inactivity during which shallow-water carbonate sedimentation took place (Piccoli, 1966; De Vecchi et al., 1976; Barbieri et al., 1982; 1991; De Vecchi and Sedea, 1995).

On the basis of different tectono-magmatic features, the Veneto Volcanic Province can be subdivided into four main volcanic districts (Figure 1): the Lessini Mountains, the Marostica Hills, the Berici Hills and the Euganean Hills. The main products are volcaniclastic rocks, hyaloclastites, pillow lavas and lava flows of a mafic to ultramafic composition. Subvolcanic bodies and rocks of more acidic compositions (up to rhyolite) only occur in the southern-most part of the region (Euganean Hills).

The Lessini Mountains extend from Mt. Baldo to the west and the Schio-Vicenza tectonic line to the east, and are located within a NNW-trending extensional structure, namely the Alpone-Agno graben or semi-graben (e.g. Zampieri, 1995; 2000), which is bounded to the west by the NNW-SSE Castelvero normal fault (Figure 1). This fault was crucial for the structural and palaeoenvironmental evolution of the Lessini Mountains in late Paleocene-middle Eocene times (Papazzoni and Trevisani, 2006), as it was a threshold separating a western area with dominant sedimentary rock and discontinuous, thin volcanic deposits from an eastern area where volcanic rocks prevail. With a thickness up to 400 m, the Lessini Mountains constitute the most representative volcanic sequence of the Veneto Volcanic Province. Volcanism is mainly characterized by tuffs and lava flows, with several column-jointing eruptive necks and subordinate hyaloclastites and pillow lavas. The most abundant rock-types are basanite and alkali olivine basalt, whereas transitional basalts, tholeiites nephelinite, hawaiites, trachy-basalt and basaltic andesites are less abundant (De Vecchi and Sedea, 1995; Tuchschmid, 1992; Milani et al., 1999; Bonadiman et al., 2001). Petrological and geochemical data from the literature (e.g. De Vecchi and Sedea, 1995; De Vecchi et al., 1976; Milani et al., 1999; Bonadiman et al., 2001; Beccaluva et al., 2001; 2007) attest that magmatism has a within-continental-plate character, in accordance with regional geodynamics, suggesting that the magmatic activity may have occurred in a tensional system as a foreland reaction to the Alpine orogenic phase. The small volumes of erupted volcanics, together with the high percentage of undifferentiated magmas spanning a wide compositional spectrum, resemble the volcanological characteristics of a low-volcanicity rift (Barberi et al., 1982).

FIELD DESCRIPTION, SAMPLING AND ANALYTICAL METHODS

The studied samples come from several localities along the Alpone Valley near Verona (Figure 1), where a thick sequence of basaltic lava flows containing a variety of secondary mineral assemblages in veins and vesicles extensively crops out. On the basis of the distribution pattern of the vesicles, three different zones can be distinguished from the base to the top of the major investigated basaltic flows: a lower, thin vesicular zone, an inner massive zone, and an upper, highly vesicular, zone. The lower zone often represents the basal part of the lava flow that is in contact with the sedimentary rocks. It consists here of a thin (up to 30 cm thick), discontinuous, vesicular interval with vesicles of less than 10 vol% that range from 1 to 5 cm in diameter. This zone grades into the massive zone that forms the central and main part of the flow. It consists of a thick (up to 20 m), massive fresh unit in which vesicles are absent or very scarce, and is often cross-cut by multiple joint sets that define narrow columns. In contrast, the upper zone is characterized by: altered facies with a huge quantity of vesicles that induce significant porosity, and important concentrations of secondary minerals. In this zone, which is 5 to 10 m thick, the abundance of vesicles seems to be inversely proportional to their average size. At the top of the flow, the vesicularity is approximately 40 vol%, with vesicle diameters from 0.1-1 cm. Meanwhile, at the base of the upper zone, the diameters of the vesicles increase to up to 20 cm and the associated porosity is in the range 5-10 vol%. These vesicles commonly interconnect to form frameworks. In the inner and upper zones, secondary minerals are also found in elongated pipe-vesicles and veins.

Secondary mineral assemblages from veins and vesicles, and their host rocks (both fresh lavas and their altered equivalents), were collected during several field trips. A large number of samples (~300) were collected in the field, sixty-five of which were analysed in detail, including twenty-one from whole rock samples and forty-four from veins and cavities for secondary mineral assemblages. Samples were petrographically studied through optical microscopy, major elements chemical analyses, X-Ray Powder Diffraction (XRPD) and Scanning Electron Microscopy (SEM).

Chemical analyses of the bulk samples were performed by the Activation laboratories (Ancaster, Canada) according to Code 4Litho package following lithium metaborate/tetraborate fusion (www.actlabs.com); quality control was carried out with the international geochemical reference standards. Weight loss on ignition (LOI) was determined by standard gravimetric techniques, after igniting the powder at ~1100 °C for 5 h. The reported LOI values are the sum of LOI+ (representative of the structural H_2O and CO_2 content) and LOI- (humidity content of the powder).

The XRPD was used to identify the very fine-grained crystals, including clay minerals. The XRPD patterns were recorded using a Philips X'Change PW 1830 X-ray diffractometer (Philips X'PERT; Cu Kα radiation). The samples were run between 2° and 70° 2θ. The analytical conditions were a 35 kV accelerating potential, a 30 mA filament current, a 0.02° step, and a counting time of 1 s/step. All of the powder samples were prepared by side-loading an aluminium holder to obtain a quasi-random orientation.

Morphology and chemical composition of the secondary minerals were investigated by a SEM Philips 515 equipped with Energy Dispersion Spectroscopy (EDS) EDAX 9900 at the University of Urbino (Italy), and a Jeol 6400 with an Oxford Link Isis located at the University of Parma (Italy). The operating conditions applied were a 15 kV accelerating potential and a 2 to 15 nA beam current.

Zeolites were analyzed with a defocused beam (20 μm) and a shortened accumulation time (from 100 s down to 50 s). Other minerals were analyzed with a beam diameter of 5 or 10 μm. Na and K were measured first, to minimize the effect of Na and K loss during determination. Natural and synthetic standards were used for calibration. The charge balance of zeolite formulas is a reliable measure for the quality of the analysis. It correlates with the extent of thermal decomposition of zeolites during microprobe analysis. A useful test is based on the charge balance between the non-framework cations and the amount of tetrahedral Al (Passaglia, 1970). Analyses are considered acceptable if the balance error $E\%=[(Al(+Fe^{3+})-Al_{theor})/Al_{theor}]\times100$, where $Al_{theor}=(Na+K)+2(Ca+Mg+Sr+Ba)$, is less than ±10% (Passaglia, 1970).

RESULTS

Composition of the host rock

Petrography

Petrographic observations were made on 21 samples. All of the studied rocks are of basaltic composition. Hydrothermal alteration is essentially made up of two components: (a) replacement of primary components in the rocks by alteration minerals, and (b) precipitation of alteration minerals into voids in the rock. Based on field and petrographic data, the samples are classified into two main types; (1) relatively fresh lavas containing very few secondary minerals (F-type), (2) hydrothermally altered lavas with clay minerals and/or zeolites (A-type). The details of the microscopic characteristics of each group are described below.

The fresh lava (F-type) samples (n=10) in the hand specimens are sub-aphanitic volcanic rock, which is black to dark grey in colour, and contain very few or no secondary minerals. Under the microscope, these samples are mainly fine-grained and weakly phyric, with a hypocrystalline to pilotaxitic texture (Figure 2 a,b). In the F-type, there is only one phenocryst assemblage of (in order of abundance) forsteritic olivine, Ca-rich plagioclase, clinopyroxene (augite) and opaques (magnetite-ilmenite), which are commonly euhedral to subhedral in shape. The groundmass is composed of plagioclase laths, anhedral olivine and clinopyroxene grains, opaque minerals such as titanomagnetite, which is locally altered to hematite, and devitrified glass with intersertal to hyalo-ophitic textures.

The hydrothermally altered lava (A-type) samples (n=11) are dark grey to light grey in colour (Figure 2 b,c). In some samples, reddish parts occur as millimeter- to centimeter-wide halos along rock margins and fracture surfaces, and a spatially restricted region (alteration halos) around the vesicles can be observed. Under the microscope phenocrysts are dominated by olivine and euhedral plagioclase (Figure 2 c,d); opaque minerals locally occur in several samples, whereas small amounts of subhedral clinopyroxene phenocrysts are recognized in only four samples. The groundmass of most of the A-type samples is commonly composed of plagioclase laths, anhedral olivine, clinopyroxene and opaque grains, locally with intergranular to sub-ophitic textures, and volcanic glass. The A-type samples are characterized by the presence of Fe-oxyhydroxide, clay minerals and zeolites. Clay minerals and Fe-oxyhydroxide, which mainly fill veins and vesicles, are greenish and brownish in colour, respectively. Microfractures in plagioclase phenocrysts are also partly lined with these minerals. Although primary igneous minerals are preserved in most of the samples, olivine phenocrysts are partly to completely replaced by iddingsite and/or yellowish clay minerals, frequently as pseudomorphs after the primary crystals. In contrast to the olivine, the clinopyroxene is very clear and shows no signs of alteration. Plagioclase (phenocrysts and microlites) is partially altered to phyllosilicates, whereas opaques are replaced by hematite. The volcanic glass is affected by alterations and replaced by clays and iron oxides. The secondary mineralogy of the A-type samples clearly indicates that they were subjected to low-temperature hydrothermal alteration (Alt et al., 1986; Teagle et al., 1996; Talbi and Honnorez, 2003). It is important to note that high- temperature alteration minerals such as chlorite, actinolite, albite, epidote, sphene, quartz and sulfides were never found in the A-type samples.

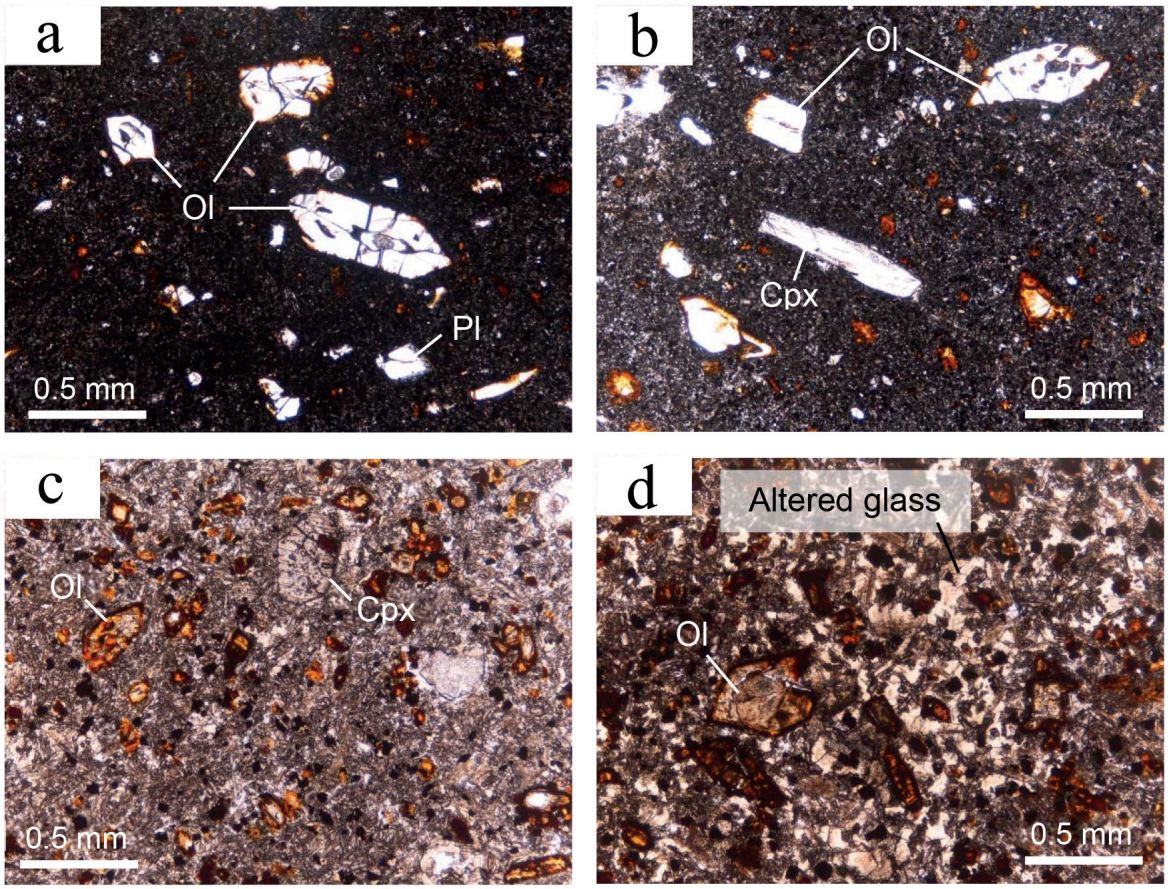

Figure 2. Photomicrographs of the tertiary basaltic rocks from the Lessini Mountains. (a,b) Weakly phyric, hypocrystalline texture in the F-type basalts. (c,d) Clay minerals replacing glass and Fe-oxyhydroxide pseudomorphs after olivine phenocrysts in the A-type basalts. Mineral abbreviations: Cpx=clinopyroxene, Pl = plagioclase.

Major elements

Bulk rock analyses of relatively fresh samples and their altered equivalents (Table 1) have been used to estimate the element budget during low-temperature hydrothermal processes.

The F-type samples appear to be relatively fresh or poorly affected by alteration, and are thus expected to retain their original chemical compositions. These samples have typical basaltic abundances of SiO_2 (45.5-46.4 wt%) and low alkali element concentrations (K_2O 1.32-1.48 wt%, Na_2O 2.64-2.82 wt%). The MgO and Cao contents are high (10.5-11.9 wt% and 9.05-10.44 wt%, respectively), the Fe_2O_3 varies from 10.04 to 11.44 wt%, while the TiO_2 is in the range of 2.22-2.65 wt%. The LOI content is low (~1.3 wt%), reflecting the lack of secondary hydrous minerals in these samples.

The SiO_2 content of the A-type (45.02-45.81.wt%, respectively) is almost the same as that of the F-type, although the former has a relatively minor decrease. Compared to the F-type, the K_2O concentrations in the A-type are slightly higher (1.59-2.01 wt%), while those of the Na_2O are relatively lower (1.12-1.43 wt%), giving the A-type rocks a basaltic composition. MgO and CaO are lower in the A-type samples (9.18-9.61 wt% and 8.23-9.46 wt%, respectively), while the TiO_2 content increases (2.87-3.43 wt%). In addition, the LOI content of the A-type samples (3.29-4.81 wt%) is significantly higher than in the F-type samples, reflecting the presence of various amounts of secondary hydrous minerals. It is important to note that the Al_2O_3 content of the A-type samples (13.18-13.87 wt%) is the same as that in the F-type versions, meaning that it can be regarded as an immobile element during the low-temperature hydrothermal processes.

Secondary mineral assemblages

Tertiary basalts from the Lessini Mountains are affected by low-temperature hydrothermal alteration. Secondary mineral assemblages are dominated by clay minerals and zeolites, with minor silica phases and calcite. On the basis

Table 1. Bulk rock composition (major elements) of relatively fresh samples (F-type) and their altered equivalents (A-type) of the Lessini basaltic rocks. LOI=Loss of ignition. Fe_2O_3 (tot)*=total iron as Fe_2O_3.

Sample Type	WR-BV6f	WR-BV12f	WR-BV14f	WR-BV6a	WR-BV612a	WR-BV614a
	F-type (massive, fresh samples)			A-type (altered samples)		
SiO_2	45.65	45.51	46.41	45.04	45.02	45.81
TiO_2	2.61	2.50	2.22	3.01	3.43	2.87
Al_2O_3	13.15	13.83	13.87	13.18	13.87	13.80
Fe_2O_3(tot)*	11.21	11.44	10.04	11.99	11.81	10.78
MnO	0.16	0.15	0.15	0.11	0.10	0.12
MgO	10.91	10.85	11.88	9.18	9.61	9.32
CaO	10.44	9.71	9.05	9.46	9.06	8.23
Na_2O	2.64	2.82	2.64	1.12	1.43	1.27
K_2O	1.32	1.44	1.48	1.59	1.87	2.01
P_2O_5	0.61	0.77	0.42	0.44	0.46	0.22
LOI	1.21	1.01	1.73	4.86	3.29	4.81
Total	99.91	100.03	99.89	99.98	99.95	99.24

of macroscopic and microscopic observations and XRPD and SEM-EDS data, three paragenetic stages can be distinguished with respect to the differences in texture and mineralogy. The textural characteristics of these stages and the sequence of mineral precipitation during each stage are shown in Figure 3.

In Stage I, concentric layers of clay and silica minerals (chalcedony and quartz) are precipitated along the inner walls of vesicles as early phases. Stage II mineralization immediately follows the Stage I products, and is characterized by the crystallization of various fine-grained zeolite species (erionite, offretite, analcime, natrolite, heulandite and stilbite). If the vesicles are very small (1-2 mm), the minerals of these stages will be the only ones to fill the space. In the case of larger voids (>1 cm), the core of the vesicles commonly contains a new generation (Stage III) of coarse-grained, well-shaped zeolites (phillipstite-harmotomo, gmelinite, chabazite, willhendersonite and yugawaralite). In addition to the minerals mentioned, calcite, when present, is generally the last mineral deposited in larger cavities. Later minerals are often deposited on corroded crystal surfaces of already-existing crystals from the previous stages.

Paragenetic Stage I: clay and silica minerals

Paragenetic Stage I is the earliest alteration in the Lessini volcanic rocks and is characterized by linings of primary pore spaces by clay and silica minerals (Figure 4). The distribution on the outcrop scale of the Stage I alteration is largely a function of the distribution of primary porosity in the lava. All the other mineral assemblages are either precipitated on top of or cross-cut the Stage I alteration phases. Clay minerals typically form layers along the walls of pore spaces with layered or botryoidal habits and appear in a wide range of colours varying from white, pink, yellow, brown and green to black (Figure 4a). Petrographic observations in the thin section reveal that clay minerals are present in three different microdomains: (1) as the earliest filling of primary voids such as vesicles and veins; (2) as pseudomorphs after primary minerals; and (3) in the groundmass replacing glass. These types of clay mineral have also been distinguished on the basis of their optical features. Type 1 minerals occur in the A-type lava as fibro-radial assemblages lining and filling the veiscles. They have an intense grass-green colour that resembles that of celadonite (Figure 4 b,c). They always precede the crystallization of zeolites in the open voids. Type 2 is colourless, has a mica-like appearance due to

high birefringence colours, and occurs as a replacement of primary phenocrysts in the A-type lava. The type 3 clay minerals have a brown to reddish-brown colour and mainly occur as groundmass replacements and rarely as vesicle fillings.

A precise identification of clay minerals requires both X-Ray powder diffraction (XRPD) studies and electron microprobe analyses as exemplified by several authors (e.g. Bettison and Schiffman, 1988; Bettison-Varga et al., 1991; Robinson et al., 1993). The XRPD patterns of the selected samples reveal a weak and broad reflection at ~14 basal spacing. With ethylene glycol treatment, this reflection becomes more distinct and sharper, and shifts to about 17 Å, suggesting the presence of smectites. The reflections at 6.41, 4.55, 3.36 and 2.59 Å with ethylene glycol correspond to saponite with a tri-octahedral structure. SEM observations of the saponite (Figure 4d) revealed a radial, petalous crystal growth, which overall takes on a globular shape or vermicular aggregates. The globules often agglutinate and the diameter of each one is about 10 to 20 microns, whereas the crystals are very small (~1-2 μm). The celadonite had a d(001) value of 9.8-10.1 Å; the d(002) peak was obscured by destructive interference, as is characteristic of high Fe micas, including celadonite

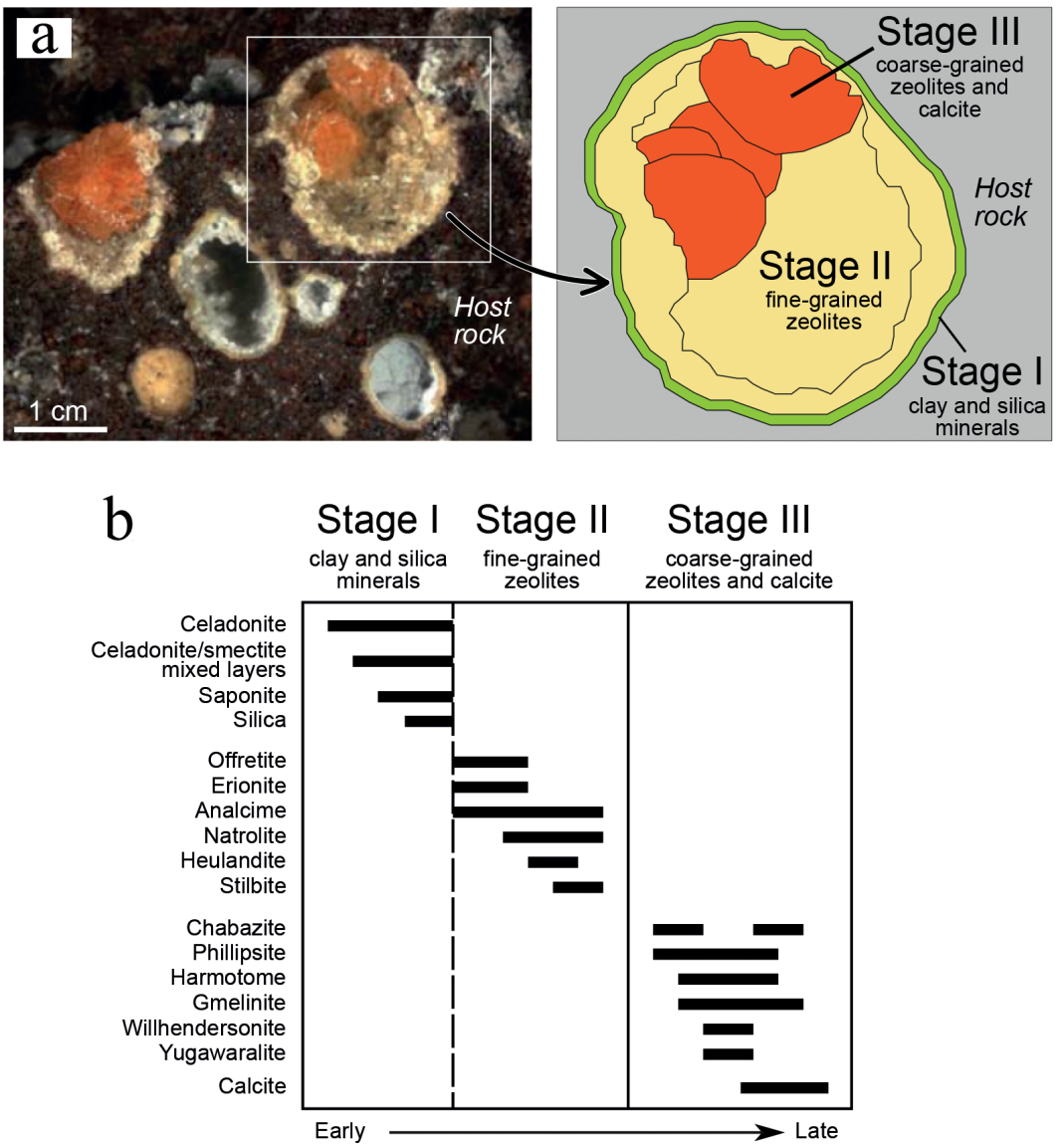

Figure 3. (a) Example of vesicles containing secondary mineral assemblages in the tertiary basaltic rocks from the Lessini Mountains and relative sketch illustrating the three recognized paragenetic stages. (b) Relative timing of mineral paragenesis and sequence of mineral precipitation during the multistage alteration processes.

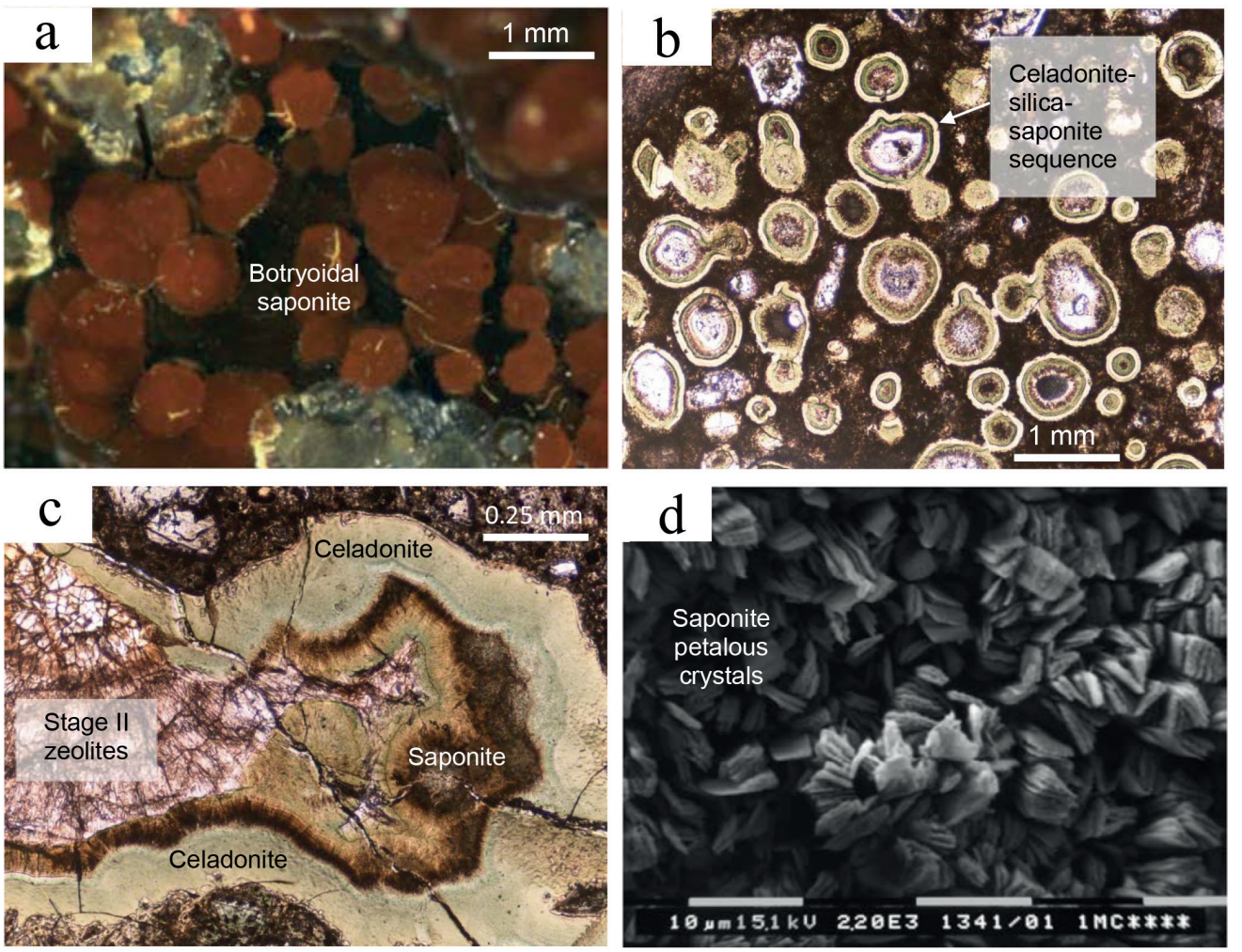

Figure 4. Photomicrographs (a,b,c) and scanning electron microscopy image (d) of the earliest Stage I alteration minerals. (a) Brownish to red tri-octahedral clay minerals (saponite) with botryoidal shape. (b) Celadonite-silica-saponite sequence along the walls of the sub-millimetric vesicles. (c) Detail of Stage I celadonite-saponite rims preceding Stage II fine-grained zeolites in a pore space. (d) Aspect of a sub-spherical globe with petalous crystal growth of clay minerals.

(Odom, 1984). The di-octahedral nature of the celadonite was indicated by its strong d(060) reflection of 1.507Å with no evidence of a 1.496 Å peak of a di-octahedral, aluminous smectite (e.g. montmorillonite). Some samples provide instances of the XRPD characteristics of the 9.8-10.1 Å phyllosilicate and celadonite, although there is evidence that a possible smectite-celadonite mixed layer mineral is present, including a weak reflection near 1.532Å that could correspond to the tri-octahedral smectite, saponite.

The chemical composition of the saponite, which is calculated by the stoichiometry of its representative composition, is $(Al_{0.03}Fe^{3+}_{1.01}Mn_{0.72}Mg_{3.83})_{5.59}(Al_{0.60}Si_{7.40})_{8.00}O_{20}(OH)_4(K_{0.02}Na_{0.04}Ca_{0.17})_{0.23}\cdot nH_2O$. The saponite contains significant amounts of Mg and Fe in octahedral sites, with mostly Ca in the interlayer sites. The saponite also has a large amount of iron and manganese and is depleted in aluminium, with a possible small cation vacancy in the octahedral site. A representative celadonite composition is $(Al_{1.35}Fe^{3+}_{2.06}Mg_{1.01})_{4.42}(Al_{0.03}Si_{7.97})_{8.00}O_{22}(OH)_4(K_{1.76}Na_{0.04}Ca_{0.05})_{1.85}\cdot nH_2O$. Stage I celadonite is close to the end-member composition defined by Buckley et al (1978), with only slightly lower K content and higher Al than the ideal end-member composition, This slight deviation could be due to the presence of a small tri-octahedral smectite component (as interstratification) in the celadonites, as also indicated by the XRPD data. The celadonite is clearly distinguished from other phyllosilicates by its distinctive green colour in both the hand specimens and the thin sections (Figure 4 b,c) and its K-rich composition.

Several chemical parameters can be used to discriminate the smectite group, the interstratified smectite/chlorite and the chlorite group, provided all the analyses have been

recalculated on the basis of the chlorite formula (i.e., 28 oxygen atoms). One of the most useful parameters is the sum of the non-interlayer cations ($Si+Al_{tot}+Fe_{tot}+Mg+Mn$), that varies from 20 for the chlorite end-member to 17.82 for the smectite end-member (Schiffman and Fridleifsson, 1991). These different poles are classically represented on a non-interlayer cation ($Si+Al_{tot}+Fe_{tot}+Mg+Mn$) vs. total Al diagram. In this diagram, the positions of the clinochlore (chlorite s.s.), saponite (trioctaedral smectite), beidellite (di-octahedral smectite) and celadonite poles were defined by Schiffman and Fridleifsson (1991), and slightly modified by Robinson et al. (1993). All the phyllosilicates analyzed in the Lessini lavas are presented in this diagram (Figure 5). All the analyses plot in a field between the saponitic and celadonitic end-members. The differences in chemistry correlate well with the petrographical types defined from the thin section studies. The mica-like clay minerals (type 2) plot near the pole of pure saponite (black triangles, Figure 5); the brown to reddish-brown clay minerals (type 3) correspond to mixed layer celadonite/smectites with a near saponitic composition (grey squares, Figure 5). The intense grass-green phyllosilicates (type 1) also correspond to a celadonite component, probably with a slight contribution of mixed-layer saponite/celadonite (white circles, Figure 5).

Silica minerals are rare and consist of quartz and/or chalcedony, and usually follow clay minerals in the crystallization sequence.

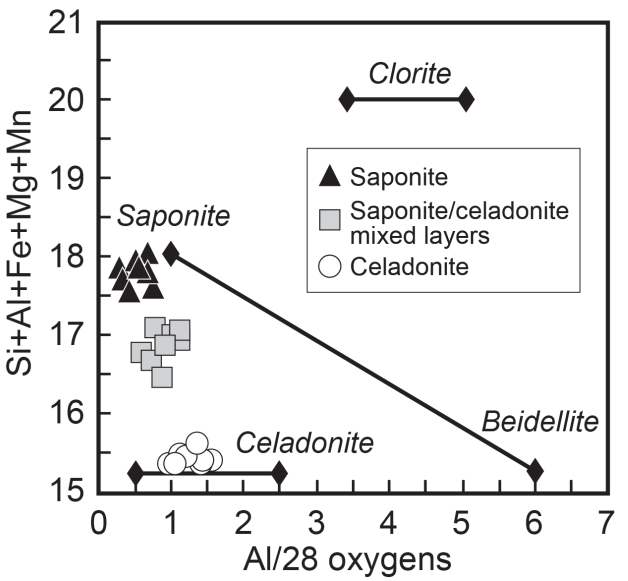

Figure 5. Non-interlayer (Si+Al+Fe+Mg+Mn) cation total vs. Al_{tot} for clay minerals from the Stage I clay minerals. End-member compositions (solid diamonds) are taken from Robinson et al. (1993).

Paragenetic Stage II: fine-grained zeolites

The paragenetic Stage I alteration is characterized by the continued infilling of primary pore spaces and the partial replacement of the groundmass and phenocryst minerals of the host rock. The Stage II mineral assemblages and paragenetic sequences are summarized in Figure 3 and illustrated in Figure 6. The typical vesicle infillings in Stage II consist of, in order of crystallization: offretite, erionite, analcime, natrolite, heulandite and stilbite. Fine-grained zeolites were normally directly precipitated on the silica and clay minerals of Stage I. Frequently, several species are present within the same vesicle, even if only one or two of these minerals can also be found. Adjacent lava flows commonly contain different mineral assemblages. In what follows, we present descriptions of their zeolite appearance, occurrences, and textural relations, as well as new chemical data on each zeolite species

Offretite

Offretite is common and occurs in different forms (Figure 6 a,b). The most frequent type is clear-white, transparent, needle-like sub-millimetric crystals, which often completely the line vesicles and vugs, although light yellow hexagonal prisms of 0.5-1 mm, which frequently form parallel aggregates, can also be found. In some samples, spherules and sub-spheric radial aggregates (up to 2 mm) of closely matted, glassy, needle-like crystals partially to completely coat the vesicle walls. Occasionally, the hexagonal prisms are surrounded by ring-shaped aggregates of clay minerals or other zeolite microcrystals such as chabazite and phillipsite-harmotome.

The average chemical composition is $Ca_{1.12}\,Na_{0.04}\,K_{0.91}\,Mg_1\,Sr_{0.02}\,Ba_{0.03}\,[Al_{5.21}\,Si_{12.77}\,O_{36}]\cdot 16H_2O$ (Table 2), with a Si/(Si+Al) ratio ranging from 0.70 to 0.72. All of the extra-framework sites are occupied by calcium (0.99-1.44 apfu), except for one sample where the dominant cation is potassium (up to 1.03 apfu); sodium is always <0.1 apfu (Figure 7). The Mg/(Ca+Na) ratio, which is considered to be the most significative parameter for the distinction between offretite and erionite (Passaglia et al., 1998), varies from 0.52 to 1.03 (Figure 8).

Erionite

Erionite occurs as clear-white to orange radiating bundles of hexagonal, needle-like to prismatic crystals of 1-3 mm in length, which are often embedded in pale-grey clay minerals or alone fill very small vesicles (Figure 6c). The crystals may be isolated or may give rise to rounded aggregates commonly radiating from a central point. Very often, the single prismatic crystals are highly elongated with a high length/diameter ratio, giving a fibrous appearance. Erionite crystals are generally colourless and transparent, but may also show slight yellowish and brownish discolourations.

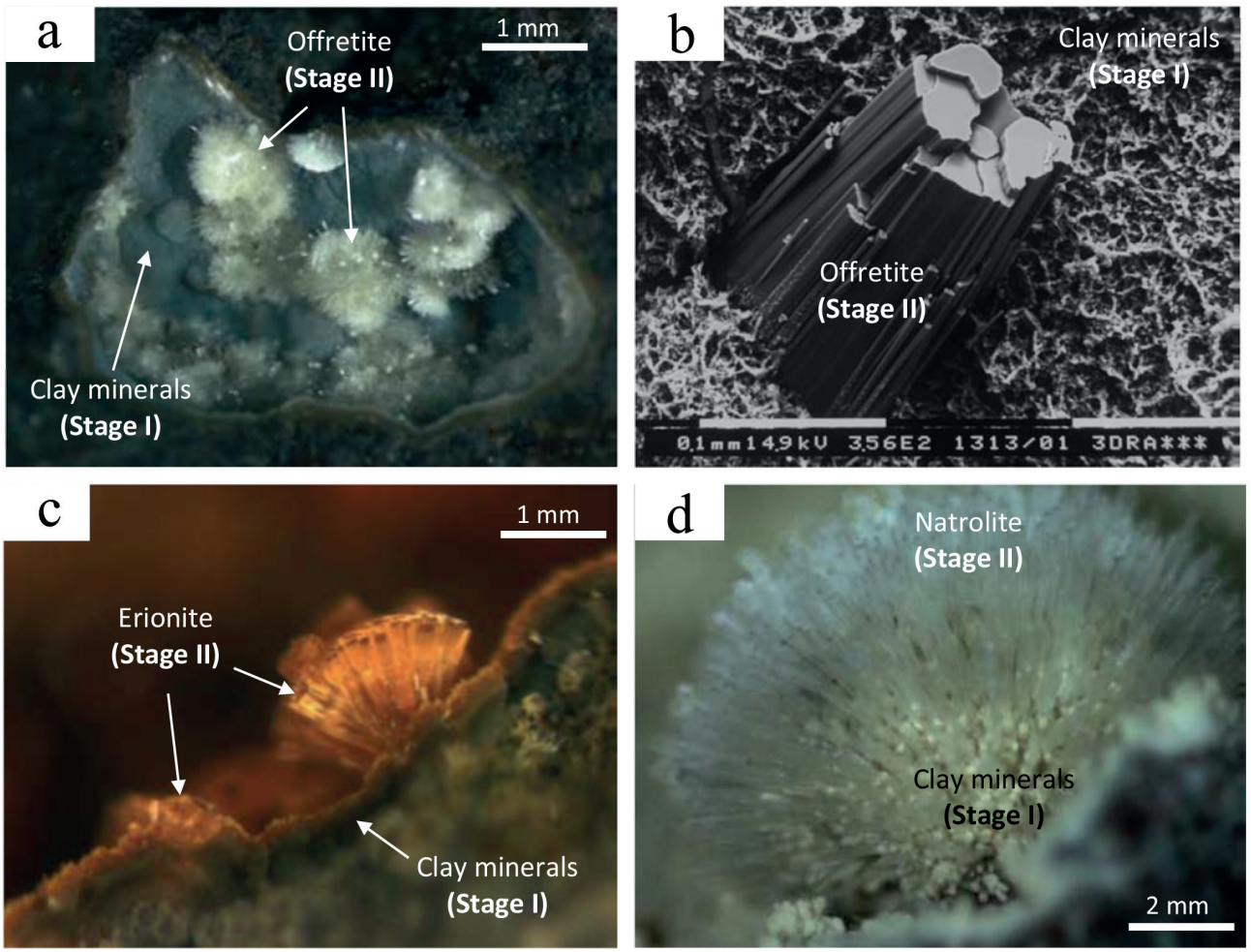

Figure 6. Photomicrographs (a,b,c) and scanning electron microscopy image (b) of the Stage II alteration minerals. (a) Sub-spheric, radial aggregates of closely matted, glassy, needle-like offretite crystals partially coating Stage I clay minerals in the vesicle walls. (b) Sub-hexagonal, prismatic to acicular offretite crystals, frequently forming parallel aggregates, surrounded by Stage I clay minerals. (c) Rounded aggregates of orange to red hexagonal crystals of erionite, commonly radiating from a central point. (d) Sub-spherical aggregate of glassy, colourless, thin prismatic crystals of natrolite radiating from a central point and grown on Stage I clay minerals.

When they come together to form rounded aggregates, the crystals often have a reddish-yellow colour and the spherical shape appears in a red-orange colour.

The average chemical composition is $Ca_{2.84}Na_{1.29}K_{2.28}Mg_{0.43}Sr_{0.09}Ba_{0.01}[Al_{10.26}Si_{25.73}O_{72}]\cdot 28H_2O$. The Si/(Si+Al) ratio is in the range 0.70-0.73, which is consistent with the literature interval for the erionite from basaltic cavities (Passaglia et al., 1998; Passaglia and Sheppard, 2001). Calcium and potassium are the dominant extra-framework cations in the structure (Figure 7). However, crystals were found in some samples in which sodium is the dominant cation, with its content also being very high (up to 2.97 apfu). Magnesium is generally very low (0.11-0.17 apfu), although in some cases reaches 0.48-0.73 apfu. The Mg/(Ca+Na) ratio is in the range 0.01-0.2 (Figure 8).

Analcime

Analcime is very common and forms well-developed, transparent to milky crystals up to 5 mm in diameter with a typical icositetrahedron {211} habit. It is usually colourless, but white, grey, pink, pale yellow, greenish and reddish crystals can also be found. More rarely, analcime is opaque, especially with the widespread presence of secondary coatings found on the surface of the crystals. It can occur either as individual crystals or as clusters in veins and cavities. Very fine-grained amygdaloidal varieties in vesicles lined with clay minerals have also been observed within the highly-altered basalts. Cavities and vein-filling analcime crystals are frequently accompanied by natrolite and phillipsite/harmotome.

The average composition of analcime is calculated as

$Na_{13.77}Ca_{0.01}K_{0.03}Ba_{0.03}[Al_{14.29}Si_{33.81}O_{96}]16H_2O$ and has a homogeneous chemical composition, with all of the extra-framework sites occupied by sodium (Table 2). The Si/(Si+Al) ratio varies from 0.70 to 0.71, which are slightly higher values than those observed in the literature for analcime from amygdales in basalts (~0.67; Passaglia and Sheppard, 2001). The Na/(Na+Ca) ratio is always ~1, as are the mono- and bivalent cation ratios. Analcime from vesicles and cavities has no differences in composition to that analyzed from fractures and veins.

Natrolite

Natrolite is very common, and can usually be found as hemispherical aggregates, up to 5 mm in diameter, with glassy, colourless to white thin prismatic crystals, which commonly radiate from a central point (Figure 6d). The crystals (up to 2 mm) are dominated by a prism with a well-formed tetragonal section, truncated by pyramids. Many of the prism faces have a very thin coating of clay minerals as botryoidal aggregates. Natrolite is often associated with analcime and phillipsite/harmotome, but can also be found as a ubiquitous phase in small vesicles.

The average chemical composition of natrolite is $Na_{14.17}Ca_{0.16}K_{0.01}[Al_{15.71}Si_{24.59}O_{80}]\cdot 16H_2O$ (Table 2), which is very close to the stoichiometric formula (Passaglia and Sheppard, 2001). The Si/(Si+Al) ratio varies from 0.59 to 0.62, while sodium is in the range 13.61-14.92 apfu and calcium is always <1 apfu.

Heulandite

Heulandite is rare in the Lessini basalts, and forms tabular, monoclinic, transparent to translucent crystals up to 2 mm in diameter. It generally occurs in thick trapezoid aggregates or clusters with a truncated blocky habit; the clusters are sometimes slightly curved. The crystals are generally colourless, but yellow to pale green colours have also been observed. In its rare occurrences, heulandite seems to post-date clay minerals and the other zeolites, and infills the inner part of the vesicles.

The average chemical composition is $Ca_{2.22}Na_{1.52}Sr_{0.33}Mg_{0.19}K_{0.16}Ba_{0.01}[Al_{7.92}Si_{28.26}O_{72}]\cdot 24H_2O$. Calcium and sodium are the dominant extra-framework cations in the structure, and because Ca is the prevailing cation, it can be classified as Ca-heulandite according to the IMA

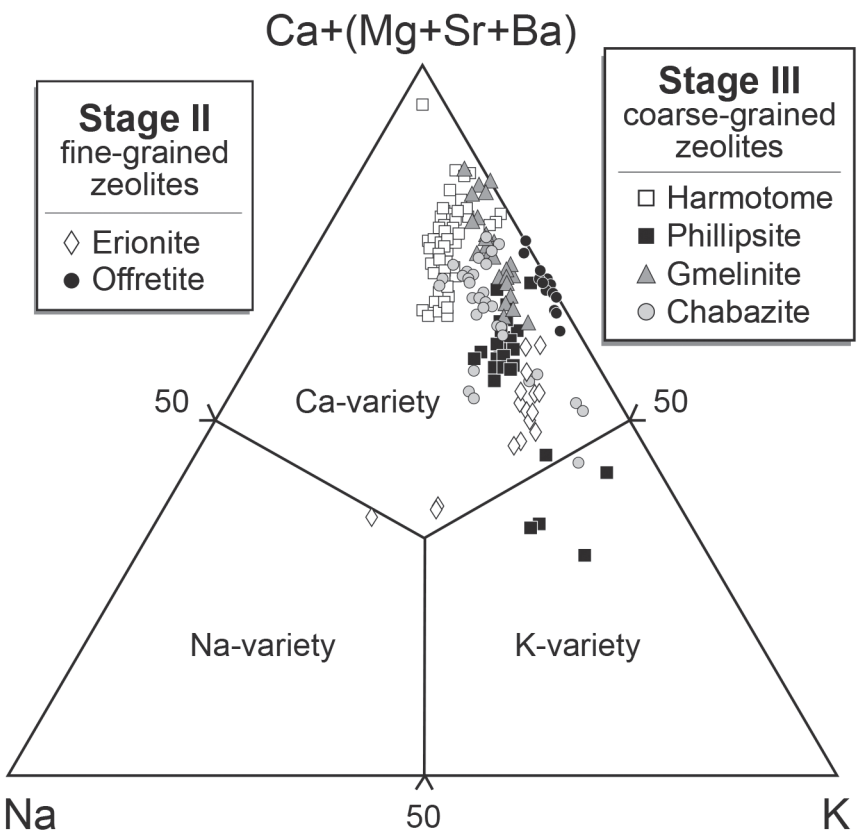

Figure 7. (Ca+Mg+Sr+Ba)-Na-K composition plot of the main zeolites from the Lessini basalts, showing the distribution of extraframework cations.

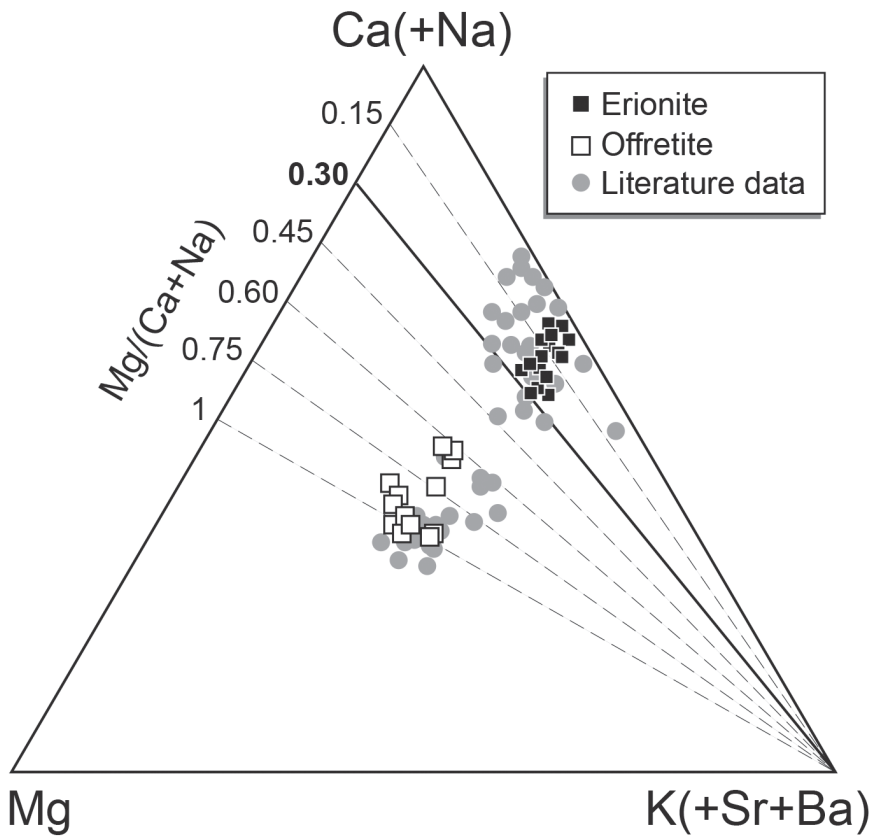

Figure 8. Compositional diagram showing the extraframework cation content of erionite and offretite from the Lessini basalts. The Mg/(Ca+Na) cation ratio, which is considered the most significant discrimination between erionite and offretite (see Passaglia et al., 1998). Literature data from other basaltic rocks (from Passaglia et al., 1998) has been reported for comparison.

nomenclature of the zeolites (Coombs et al., 1998). The Si/(Si+Al) ratio is in the range 0.77-0.81, whereas strontium, magnesium and potassium are present as minor cations.

Stilbite

Stilbite is rare and occurs as thick, tabular to lamellar crystals with pointed terminations that range from 0.1 to 1 mm in size. The crystals often grow wider towards the end, forming sheaf-like aggregates. Stilbite is generally milky-white, but clear and translucent variants also exist, as do coloured types, which are usually pale yellow to reddish. Stilbite is accompanied by other zeolites such as chabazite and phillipsite-harmotome.

The average chemical composition of stilbite is calculated as $Ca_{2.55}Na_{1.51}Sr_{0.78}K_{0.10}Mg_{0.05}Ba_{0.03}[Al_{9.2}Si_{26.99}O_{72}]\cdot 30H_2O$. The sodium and calcium content ranges from 1.11 to 1.02 and from 3.38 to 4.44 apfu, respectively. The average Si/(Si+Al) ratio is 0.76.

Paragenetic Stage III: coarse-grained zeolites and calcite

The latest alteration phase in the Lessini basalts (Stage III) is well developed in the large primary vesicles and secondary pore space (fractures and veins). The Stage III mineral assemblages are represented by coarse-grained (mm- to cm- scale), euhedral zeolite crystals that were normally grown on the fine-grained crystals of Stage II (Figure 3). They represent the final phases to crystallize in the vesicles and vugs of the Lessini basalts, followed only by calcite. The Stage III zeolite species (Figure 9) occur in the following order in the vesicles: chabazite, phillipsite, harmotome, gmelinite, willhendersonite and yugawaralite. For the latter (willhendersonite and yugawaralite), this is the first occurrence in the Lessini Mountains.

Chabazite

Chabazite is one of the most common zeolites filling cavities and vesicles within the Lessini volcanic rocks, and is also one of the minerals that have the most varied morphologies (Figure 9 a,b). Chabazite typically occurs as smooth, colourless to milky-white, perfect rhombohedral crystals of 0.1 to 2 mm in size, commonly forming

multiple, interpenetrating aggregates with sub-spherical morphologies. In places, it has pseudo-cubic forms that are often twinned. More rarely, chabazite occurs as glassy, colourless to pinky, yellow and orange crystals that usually interpenetrate, forming lens-shaped aggregates up to 5 mm in diameter that are more ("phacolitic" habit) or less ("herschelitic" habit) rounded due to complex twinning (Akizuki and Konno, 1987; Akizuki et al., 1989). In the Lessini basalts, chabazite is also present as crystals (1-3 mm in diameter), with tabular morphologies resulting from the stacking of thin, pseudo-hexagonal lamellae, which are very similar to those described by Akizuki et al. (1989) for some chabazites from Aci Castello, Sicily. Chabazite is generally accompanied by phillipsite/harmotome, erionite-offretite, gmelinite and, rarely, willhendersonite, but can also occur as a single zeolite species in vesicles and cavities that are lined with clay minerals.

The average chemical composition calculated from the SEM-EDS analyses based on 24 oxygen atoms is $Ca_{1.12}Na_{0.18}K_{0.57}Sr_{0.09}[Al_{3.38}Si_{8.61}O_{24}]\cdot 12H_2O$, and the different habits vary significantly in composition (Table 2). The Si/(Si+Al) ratio, which is the percentage of the tetrahedral framework sites occupied by Si, has its highest values for rhombohedral crystals and sub-spherical aggregates (0.72-0.74), whereas it ranges from 0.69 to 0.70 in crystals with tabular morphologies. Calcium is the most dominant extra-framework cation (1.14-1.36 apfu), except for tabular crystals, which have similar calcium and potassium contents (0.88-1.20 and 0.89-1.19 apfu, respectively). Unlike what is reported in the literature (Passaglia, 1970; Birch, 1988; 1989; Wise and Kleck, 1988; Akizuki et al., 1989; Vezzalini et al., 1994), Ca also dominates in samples displaying "herschelitic" and "phacolitic" habits. It is important to note that the tabular crystals are characterized by significant Sr content (0.16-0.32 apfu), with values greater than the average values normally reported in the literature, and comparable with those observed in chabazites found in cavities of basaltic rocks of the Plateau des Coirons, Ardeche, France and in Roman leucitites (Passaglia, 1970; Robert, 1988). Taken as a whole, according to the literature (Coombs et al., 1998; Passaglia and Sheppard, 2001), the chabazites in the Lessini basalts can be classified as Ca-chabazites (Figure 7).

Phillipsite-harmotome

According to the literature (Passaglia and Sheppard, 2001), on the basis of structural and crystallochemical data, phillipsite and harmotome can be described as a single zeolite species. Samples with K/(K+Ba)>0.50 (i.e. K>Ba) will be described as phillipsite, whereas those with K/(K+Ba)<0.50 (i.e. Ba>K) will be characterized as harmotome. Phillipsite-harmotomes are also very common within Lessini volcanic rocks and occur in a variety of forms (Figure 9 c,d). They can usually be found as lustrous, glassy, short prismatic crystals of 0.5-2 mm in size, generally forming dense, interpenetrating crystal aggregates. In places, these crystals are parallel-aligned contact twins consisting of three individual fourling twins. Phillipsite-harmotome can also occur as linings of densely matted tiny crystals that completely line vesicles and vugs, or as spherules and botryoidal radial aggregates (up to 5 mm) of closely matted, glassy, prismatic crystals that completely coat vesicle walls. They are usually associated with chabazite, erionite/offretite, natrolite and analcime. Chemical analyses performed on several crystals of phillipsite-harmotome from the Lessini volcanic rocks revealed a highly variable composition and showed the presence of crystals with almost pure compositions, as well as those with a range of intermediate compositions. This further confirmed the existence of a complete miscibility between the two end-members phillipsite and harmotome, as already suggested by several authors (Cerny et al., 1977; Tschernich and Wise, 1982; Passaglia and Bertoldi, 1983; Robert, 1988; Hansen, 1990; Armbruster et al., 1991; Passaglia and Sheppard, 2001).

Phillipsite is much more common than harmotome in the Lessini volcanic rocks, and its average chemical composition is $Ca_{1.4}Na_{0.34}K_1Ba_{0.27}[Al_{4.67}Si_{11.31}O_{32}]\cdot 12H_2O$ (Table 2). The Si/(Si+Al) ratio ranges from 0.68 to 0.78, whereas the Na/(Na+Ca) and K/(K+Ba) ratios are in the range of 0.04-0.37 and 0.59-1 apfu, respectively. The dominant extra-framework cations are potassium and calcium, which vary from 0.64 to 2.09 and from 0.99 to 1.65, respectively (Figure 6). Other cations are absent or very low. Harmotome has an average chemical composition of $Ca_{1.01}Na_{0.21}K_{0.37}Ba_{0.87}[Al_{4.52}Si_{11.14}O_{32}]\cdot 12H_2O$ (Table 2), with a Si/(Si+Al) ratio ranging from 0.70 to 0.73, a K/(K+Ba) ratio between 0.02 and 0.46, and a Na/(Na+Ca) ratio from 0.03 to 0.74. Barium and calcium are the dominant extra-framework cations (0.42-1.84 and 0.72-1.51 apfu, respectively), whereas potassium is low (0.25-0.70 apfu) and other cations are always <1 apfu (Figure 7). It is important to note that the different chemical compositions of phillipsite and harmotome do not correspond to particular differences in morphology and other physical properties. However, spherules and botryoidal radial aggregates usually correspond to barium-rich compositions, whereas transparent, colourless individual crystals frequently match the phillipsite pure member.

Gmelinite

Gmelinite occurs as single crystals or as groups of intergrown crystals (Figure 9 e,f). It is typically granular, translucent and colourless, although rare pink, yellowish, orange and red coral crystals were observed. The crystals (as large as 1 mm in size) display a typical hexagonal dipyramid modified by a first order prism and basal

Table 2. Representative chemical compositions (average and range) of the main zeolites from the Lessini Mts.

	Chabazite		Phillipsite		Harmotome	
	average	range	average	range	average	range
	n = 10		n = 15		n = 12	
SiO_2	56.24	54.06-57.49	54.30	51.77-56.07	53.67	52.85-54.39
Al_2O_3	18.71	17.21-20.62	18.31	17.16-19.27	18.56	17.6-19.24
Fe_2O_3*	0.04	0.03-0.07	0.07	0.01-0.12	0.05	0.01-0.11
MgO	0.62	0.07-0.95	0.04	0.03-0.06	0.05	0.09-0.1
BaO	0.09	0.09-0.3	4.26	3.24-5.29	9.19	4.97-12.43
SrO	1.00	0.32-2.33	0.09	0.03-0.15	0.11	0.10-0.12
CaO	6.81	5.37-7.8	5.86	4.93-6.46	4.93	0.06-0.12
Na_2O	0.61	0.24-0.98	1.17	0.35-2.34	0.49	0.13-1.19
K_2O	2.89	1.76-6.07	2.62	1.713.87	1.37	0.93-1.84
H_2O	13.01	10.63-15.25	13.42	10.4-18.75	11.68	9.72-14.77
Total	100.00		100.13		100.11	
Basis	24 oxygens		32 oxygens		32 oxygens	
Si	8.61	8.29-8.84	11.44	11.29-11.61	11.42	11.27-11.57
Al	3.38	3.14-3.73	4.55	4.42-4.68	4.65	4.53-4.8
Fe	0.01	0.01-0.02	0.01	0.01-0.02	0.01	0.01-0.02
Mg	0.14	0.02-0.22	0.02	0.01-0.02	0.02	0.01-0.03
Ba	0.01	0.01-0.02	0.35	0.27-0.42	0.77	0.42-1.06
Sr	0.09	0.03-0.21	0.02	0.02-0.02	0.02	0.01-0.02
Ca	1.12	0.88-1.25	1.32	1.15-1.41	1.12	0.72-1.51
Na	0.18	0.07-0.28	0.48	0.14-0.98	0.20	0.05-0.49
K	0.57	0.35-1.19	0.71	0.45-1.05	0.37	0.25-0.5
E%	-2.30		-1.10		5.20	
R	0.72	0.69-0.74	0.72	0.71-0.72	0.71	0.7-0.72
M/(M+B)	0.36	0.25-0.56	0.41	0.24-0.53	0.23	0.14-0.35

Note: n=number of analyses; E% (balance error)={[Al(+$Fe3^+$)-Altheor]/Altheor}×100, where Altheor=(Na+K)+2(Ca+Mg+Sr+Ba), according to Passaglia (1970); R=Si/(Si+Al); M/(M+B)=(Na+K)/(Na+K+Ca+Mg+Sr+Ba); - =analysed but below detection limit. Fe_2O_3 (tot)*=total iron as Fe_2O_3.

pinacoids. Many of the crystals exhibit the effects of dissolution that appears: to have started from the prism and dipyramid faces, and to have removed much of the interior of the crystal. Associations of gmelinite, chabazite and phillipsite/harmotome are very common.

Gmelinite from the Lessini basalts is very homogeneous, and its average chemical composition is $Na_{0.19}Ca_{2.63}K_{0.86}[Al_{6.66}Si_{17.25}O_{48}]\cdot 22H_2O$ (Table 2). The Si/(Si+Al) ratio varies from 0.72 to 0.73, which is slightly higher than the average literature data (0.69, Passaglia and Sheppard, 2001), but similar to the ratios described for the surrounding areas (Montecchio Maggiore, Passaglia et al., 1978; Luppi et al., 2007). Calcium is notably high and represents the dominant extra-framework cation (1.93-2.84 apfu), whereas potassium is low (0.55-1.23 apfu) and the other cations are always <1 apfu (Figure 7).

Willhendersonite

Willhendersonite is also very rare and occurs as transparent, colourless, rectangular laths (up to 0.3 mm in length) in a few cavities of the upper zone of the basaltic lava flows. The individual crystals are flattened and often grow together to form small groups with irregular, elongated morphologies. It can also be found with chabazite.

The average chemical composition of willhendersonite is $Ca_{2.08}Na_{0.17}K_{1.75}Sr_{0.02}[Al_{5.94}Si_{6.13}O_{24}]\cdot 10H_2O$. The Si/(Si+Al) ratio ranges from 0.5 to 0.52; calcium is the dominant extra-framework cation (2.06-2.09 apfu),

Table 2: continued…

	Analcime		Natrolite		Gmelinite		Offretite	
	average	range	average	range	average	range	average	range
	n = 9		n = 7		n = 10		n = 9	
SiO_2	58.70	57.94-59.29	49.01	47.7-50.46	55.35	54.31-56.84	53.41	50.88-57.3
Al_2O_3	21.05	20.78-21.31	26.58	25.82-28.27	18.14	17.33-18.51	18.51	17.53-19.89
Fe_2O_3*	-	-	-	-	0.06	0.01-0.11	0.14	0.01-0.36
MgO	-	-	-	-	0.22	0.01-0.69	2.81	2.17-3.25
BaO	0.25	0.18-0.37	-	-	0.27	0.04-0.88	0.25	0.03-0.67
SrO	-	-	-	-	1.30	0.38-6.08	0.10	0.01-0.15
CaO	0.03	0.01-0.09	0.30	0.01-0.85	7.88	5.78-8.47	4.38	3.79-5.69
Na_2O	12.33	11.89-12.74	14.57	13.99-15.33	0.30	0.02-0.54	0.09	0.03-0.19
K_2O	0.04	0.01-0.08	0.03	0.01-0.04	2.16	1.4-3.16	2.96	2.25-3.3
H_2O	7.68	6.76-8.89	9.37	7.23-11.14	14.47	11.91-16.77	17.51	12.49-19.83
Total	100.09		99.85		100.14		100.15	
Basis	96 oxygens		80 oxygens		48 oxygens		36 oxygens	
Si	33.81	33.72-33.94	24.59	23.99-25.19	17.25	17.16-17.37	12.77	12.52-12.95
Al	14.29	14.13-14.53	15.71	15.19-16.48	6.66	6.48-6.77	5.21	5.02-5.49
Fe	-	-	-	-	0.02	0.01-0.03	0.03	0.01-0.07
Mg	-	-	-	-	0.10	0.01-0.32	1.00	0.76-1.1
Ba	0.05	0.01-0.08	-	-	0.03	0.01-0.11	0.03	0.01-0.07
Sr	-	-	-	-	0.24	0.07-0.24	0.02	0.01-0.02
Ca	0.02	0.01-0.06	0.16	0.01-0.47	2.63	1.93-2.84	1.12	1.06-1.43
Na	13.77	13.42-14.24	14.17	13.69-14.92	0.19	0.01-0.32	0.04	0.01-0.09
K	0.03	0.01-0.06	0.02	0.01-0.02	0.86	0.55-1.23	0.91	0.7-1.03
E%	2.50		8.20		-5.20		-0.90	
R	0.70	0.70-0.71	0.61	0.59-0.62	0.72	0.72-0.73	0.71	0.70-0.72
M/(M+B)	0.99	0.96-1	0.99	0.97-1	0.26	0.16-0.34	0.30	0.25-0.36

potassium is significant (1.71-1.79 apfu), and the sodium is always <0.2 apfu. These compositions are comparable with those reported by Vezzalini et al. (1997) for the willhendersonite from Colle Fabbri, Terni (Italy).

Yugawaralite

Yugawaralite is extremely rare and was only found in two samples, where it forms transparent, colourless platy crystals with oblique ends that are morphologically very similar to those described by Eberlein et al. (1971) and Pongiluppi (1977). Yugawaralite crystallizes as distinct zeolite directly on clay minerals, or is found in association with transparent, flattened phillipsite-harmotome, making it very difficult to distinguish between these two zeolites.

The average chemical composition of Yugawaralite is $Na_{0.02}Ca_{1.97}[Al_{3.97}Si_{12.03}O_{32}]\cdot 16H_2O$, which is very similar to the literature compositions (Passaglia and Sheppard, 2001). The Si/(Si+Al) ratio is ~0.75, and calcium is the only extra-framework cation present; the sodium levels are negligible (<0.2 apfu), whereas other extra-framework cations are absent.

Calcite

Calcite is very common in the vugs of the Lessini basalts and can be found as single, large, isolated crystals, and as associated individuals or in a massive form. The single crystals are usually colourless, transparent to translucent and have rombohedral morphologies that are more or less flattened along the c axis. Prismatic crystals terminated by rombohedra were also observed, whereas calcite as granular masses or coralloid morphologies is very common. The dominant colour is white, but it can also be found in pale-yellow and pink.

DISCUSSION

Most of the ancient volcanic rocks outcropping on the Earth's surface are affected to alter by various agents, including hydrothermal fluids and groundwater. The specific reactions that occur between volcanic rocks and groundwater and/or hydrothermal fluids are mainly dependent on temperature-pressure conditions as well as the composition of the host rock and fluids (e.g. Kristmannsdóttir and Tómasson, 1978; Neuhoff et al., 1999; 2000; Weisenberger and Bucher, 2011; Kousehlar et al., 2012; Weisenberger et al., 2014). For example, in the case of basaltic rocks, their primary magmatic phases (olivine, pyroxene, anorthite-rich plagioclase, oxides and glass) become metastable and undergo extensive dissolution and hydrolysis. This results in the release of the chemical constituents of volcanic rocks such as clays and zeolites into the aqueous phase, and these eventually precipitate as secondary phases. In the following we will discuss (i) the assemblages and paragenetic sequences of the secondary minerals in the Lessini basalts, (ii) their genetic relationships with the host rocks on the basis of the chemical exchange, and (iii) their alteration conditions and mechanism.

Secondary mineral assemblages and paragenetic sequence

Alteration of the basaltic rocks in the Lessini Mountains. resulted in distinctive secondary mineral assemblages that represent a multi-stage hydrothermal alteration process. The occurrence of secondary minerals and their frequency in the studied rocks is not homogeneous, and their associations may be significantly different on both the outcrop- and sample-scale, with a variability that can be in the order of a few centimeters. In places, the mineralogical assemblages vary in a completely random way, and factors were not observed (at least on the outcrop scale) that may have acted as possible control elements for the different assemblages. In many other places, however, the assemblages are progressive and regular, and can be found in a widespread area.

By comparing all of the detailed systematic observations of the secondary mineral assemblages, three main paragenetic stages can be recognized during the alteration processes in the Lessini basalts. The earliest alteration phase (Stage I) is characterized by linings of the primary pore space by celadonite and silica minerals, and later by tri-octahedral smectites (saponite). Phyllosilicates as well as chalcedony and quartz typically form layers along the walls of the pore space with a layered or botryoidal habit. The paragenetic Stage II is dominated by fine-grained zeolites including Ca-dominated species (erionite, offretite, heulandite and stilbite) and pure Na-zeolites (analcime and natrolite). The minerals of Stage II seem to have precipitated directly on those of Stage I, and no evidence of a break between the two stages has been found. The latest stage (Stage III) is characterized by the growing of well-formed, coarse-grained zeolites and later by calcite crystals. All the zeolite species formed in the the Stage III are Ca-dominated (phillipstite-harmotomo, gmelinite, chabazite, willhendersonite and yugawaralite). Later minerals are, with very few exceptions, deposited on the corroded crystal surfaces of already-existing crystals from the previous stages, suggesting the presence of a significant interruption in the crystallization process between Stage II and Stage III.

Stages I and II show a progressive change in their paragenesis from phyllosilicates+quartz to assemblages dominated by Ca- and Na-zeolites. This paragenetic trend was probably coincident with gradual changes in temperature and pressure. However, the abrupt shift in the mineral composition from clay minerals and silica to zeolites seems to reflect a chemical evolution of the solutions from which these minerals precipitated. Celadonite precipitate in oxidative conditions in the most sensitive microsites (olivine crystal and the wall-rock periphery of the vesicles), whereas saponite is more widespread (as pseudomorphs, in mesostasis sites and within vesicles). The observed paragenetic trend (from mafic phyllosilicates to Ca- and Na-zeolites), is consistent with the results of experimental simulations of basalt-meteoric water interactions at low temperatures. Ghiara et al. (1993) showed that experiments on the closed-system dissolution of basaltic glass at low temperatures resulted in a mineral paragenesis of early smectite + phillipsite followed by analcime. During these experiments, the Mg concentrations in the solution increased rapidly at the start, and then failed as the Mg-rich smectite precipitated. The calcium concentrations also rose rapidly during the initial stages of these experiments, and continued to increase until the latter stages, when the fluids evolved towards the stability fields of the Na-zeolites. Similar experiments by Gìslason and Eugster (1987a) on the dissolution of basaltic glass and crystalline basalt at 25 °C, 45 °C, and 65 °C produced almost identical results, i.e. the zeolite paragenesis in Stage II corresponds to a decrease in the Ca/Na ratio, as well as an increase in the Si/Al ratio.

In contrast, the transition from Stage II to Stage III exhibits pronounced textural and mineralogical changes. The grain of the zeolite crystals abruptly increases from fine to coarse, their compositions become only Ca-dominated, and a latest, extensive crystallization of calcite occurred. This sudden change is also evidenced by the fact that Stage III zeolites are often deposited on corroded crystal surfaces of Stage II crystals. As a consequence, the zeolite-filled vesicles and veins of Stage III were probably related to a new, probably different, alteration phase.

Chemical exchange during alteration

The effects of alteration on the bulk rock composition can be assessed by comparing the fresh or relatively unaltered samples (F-types) with examples of altered samples

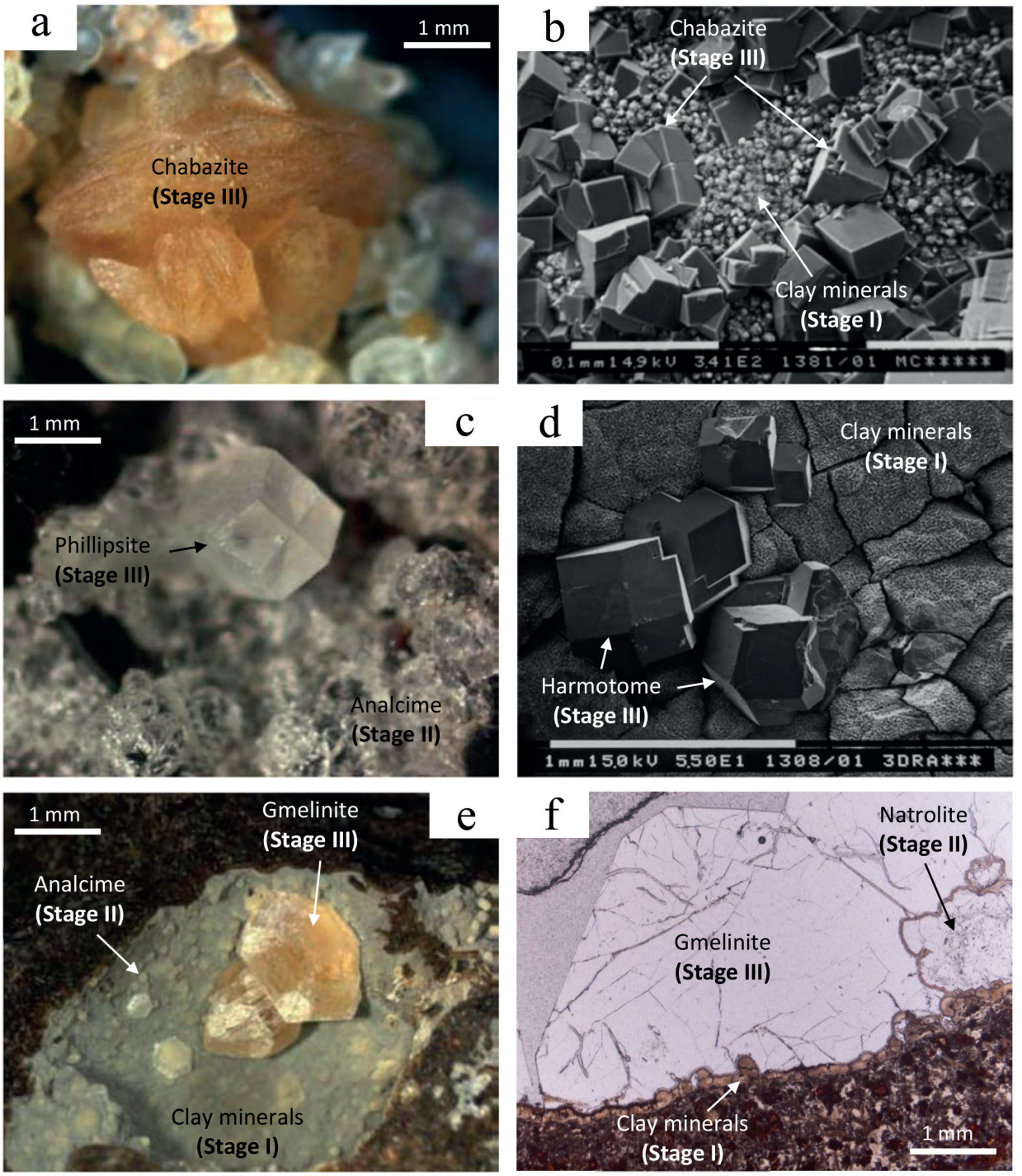

Figure 9. Photomicrographs (a,c,e,f) and scanning electron microscopy image (b,d) of the latest Stage III alteration minerals. (a) Yellow crystals of chabazite with complex twinning forming a rounded aggregate with "herschelitic" habit. (b) Perfect rhombohedral to pseudo-cubic chabazite crystals, commonly forming multiple, interpenetrating aggregates. (c) Well-shaped, transparent phillipsite crystal consisting of two sets of penetration twins, grown on Stage II fine-grained analcime. (d) Harmotome twinned crystals grown on Stage I clay minerals. (e) Yellowish crystals of gmelinite exhibiting the typical hexagonal dipyramid modified by a poorly developed, first order prism and a basal pinacoid, grown on Stage II analcime and Stage I Clay minerals. (f) Gmelinite crystals partially grown on Stage II natrolite and Stage I clay minerals.

(A-types) from the same flows. In this study, element gains and losses during alteration are estimated starting with the isocon method of Grant (1986). This method has been simplified here and applied without a quantitative estimation of changes in mass during mass transfer, by using a simple graphical visualization of altered versus original compositions. According to Nakamura et al. (2007) elements that have remained immobile during the alteration process define the isocon and plot on a straight line through the origin. Data points lying around the isocon, as defined by the elements considered to be immobile, represent either a mass gain or a mass loss depending on whether they fall, respectively, above or below the isocon.

For the studied samples from the Lessini Mountains, the simplified isocon diagram is shown in Figure 10a. The Al behaves as a relatively immobile element, as also reported by many authors for various hydrothermal systems (e.g. Winchester and Floyd, 1978; Jiang et al., 2005; De Palomera et al., 2012; Mattioli et al., 2014), and we have thus used it to define the isocon (labelled "constant mass isocon" in Figure 10a) for mass change estimations. With this isocon, samples representing the A-type basalts show that alteration was accompanied by enrichment in K_2O, TiO_2 and LOI and the depletion of Na_2O, MnO and Mg (Figure 10a). The Fe_2O_3 and CaO data fall slightly above and below the isocon, respectively. In order to quantify the geochemical exchange during alteration, the enrichment factor was calculated using the following relationship:

$$Ex = (Fx/F\mathrm{Al_2O_3})/(Ax/A\mathrm{Al_2O_3})$$

where Ex is the enrichment factor of the element X, Fx and Ax are the concentrations of element X in fresh and altered samples, respectively, and $F\mathrm{Al_2O}$ and $A\mathrm{Al_2O_3}$ are the Al_2O_3 contents in fresh and altered samples, respectively. In Figure 10b, the average enrichment factors of the major elements in the F- and A-types are presented. This diagram clearly shows the addition or depletion of each element during alteration, confirming what has previously been observed. The A-type is characterized by the enrichment of LOI, K_2O and TiO_2, while elements such as Na_2O, MnO and MgO are depleted. The A-type also shows a small increase in Fe_2O_3 and a decrease of CaO. The concentration of SiO_2 is almost the same in the F-type.

The depletion of Na_2O and CaO and the enrichment in K_2O during alteration may be related to the destabilization of the feldspars to form sericite. The presence of K-rich celadonite, which is commonly recognized in the A-type samples (Stage I), is also responsible for the K_2O enrichment. On the other hand, potassium is very mobile during the near-surface alteration of basaltic lava (Neuhoff et al., 1999). The CaO-depletion in the A-type samples may also be attributed to the alteration of Ca-bearing phases such as clinopyroxene and glass. The small increase in Fe_2O_3 reflects the oxidation of the ferromagnesian minerals (e.g. olivine). Mg-enrichment, which is one of the typical features of high-temperature, hydrothermally-altered basalts (e.g. Mottl, 1983), has not been observed in the A-type Lessini samples. Moreover, a chemical contribution to the crystallization of the secondary minerals may also be derived directly from the alteration of basaltic glass. Several authors (e.g. Eggleton and Keller, 1982; Karrat et al., 1998; Weisenberger and Spurgin, 2009) have clearly show that chemical elements like Mg, Ca, Na, K, Al and Si were mobile during the alteration processes of basaltic glass. By comparing the mobility of the chemical elements of the host rock during the alteration processes with the chemistry of the secondary mineral phases, it can be suggested that the chemical components necessary to precipitate the vesicle-filling minerals (at least those of Stage I and Stage II) may be derived from the alteration of host rocks. The extensive precipitation of phyllosilicates, silica minerals, and fine-grained zeolites in pore spaces during stages I and II indicates that Si, Al, Ca, Na, K, Fe, and Mg were mobile over scales of a millimeter or more. This is also indicated by the presence of a spatially-restricted region (alteration haloes) around the vesicles over which diffusion processes can occur. The textural preservation of pore walls and the successive lining of pore spaces during mineral paragenesis, which requires the chemical components that are necessary for the precipitation of secondary minerals to be transported into the pores, further support this hypothesis. All the components that are necessary to form the mineral assemblages of the two earlier Stages I and II were readily available in the primary phases in the lava (glass, olivine, plagioclase and pyroxene). Conversely, textural and mineralogical evidences of the Stage III alteration are coherent with a significant change in the conditions of the crystallization, and suggest the presence of new, possibly external, fluids that move within the basaltic rocks during this later phase of hydrothermal alteration. These late-stage fluids are probably enriched in Ca and $(CO3)^{2-}$ and led to the extensive crystallization of Ca-rich zeolites and calcite of the Stage III.

Alteration conditions and mechanism

Zeolites within basaltic lava are often indicative of a low-grade regional metamorphism (e.g., Walker, 1960a; 1960b; Gianelli et al., 1998; Neuhoff et al., 1999; Schenato et al., 2003; Weisenberger and Selbekk, 2008; Kouselhar et al., 2012). Nevertheless, most zeolites crystallize rapidly also in a low temperature range (40-250 °C) and a water-rich environment (Kristmannsdottir and Tomasson, 1978). In experiments on the basalt–seawater interaction, smectites (usually iron-rich saponites) are commonly produced at temperatures <150 °C (Seyfried and Bischoff, 1979;

Gianelli et al., 1998). In several hydrothermal systems di- and tri-octahedral smectite are transformed at 200-240 °C into C/S mixed layers and corrensite., which are the predominant layer silicates in the temperature range of 245-265 °C. At higher temperatures, chlorite is the most abundant clay mineral, with minor C/S mixed layers. In the Lessini basalts, evidence has never been found of sub-greenschist facies alteration products such as medium- to high-temperature zeolites, chlorite and interstratified chlorite–smectite mixed layers, among other mafic phyllosilicates (Schiffman and Fridleifsson, 1991; Neuhoff et al., 1999; Weisenberger and Selbekk, 2009). Regional metamorphism in low-grade (zeolite facies) conditions, as defined by Coombs et al., (1959), should have also resulted in regional zeolite zonation, but such zoning has not been recognized in the present study. Likewise, no geological evidence of the regional burial metamorphism of the Lessini volcanics has been found.

Experimental data on zeolite formation from basaltic starting materials indicate that chabazite and phillipsite are stable in the temperature range between 50-100 °C and 50-150 °C, respectively (Kristmannsdottir and Tomasson, 1978; Holler and Wirsching, 1988; Barth-Wirsching and Holler, 1989; Bish and Ming, 2001; Deer et al., 2004). Senderov (1988) showed that analcime and natrolite are stable in Si-deficient systems, with temperatures up to 250° C (natrolite) and 350° C (analcime). Consequently, the precipitation of these zeolites from solutions is not linked to the thermal conditions of the system, but mainly depends on other factors (e.g. the activity of the silica). Very limited data is available in the literature about the genetic conditions of erionite and offretite. Ueda et al. (1985), in an experimental piece of work, achieved the precipitation of these zeolites from a gel to a temperature of about 100 °C.

According to this evidences, and on the basis of the collected data, the secondary mineral assemblages observed in the Lessini basalts, including zeolites and mafic phyllosilicates (celadonite and saponite), were formed during the interaction of fluids with the already-solidified host rocks in low-temperature conditions at the Earth's surface. Rogers et al. (2006) estimated temperatures not exceeding 80 °C for similar mineral assemblages in W Greenland, comparing them with the occurrence at County Antrim, Ireland (Walker, 1960a; 1960b). The mineral paragenesis analcime and natrolite in W Greenland corresponds to temperatures of less than 100 °C (Neuhoff et al., 2006). Therefore, the temperature for zeolite formation in the Lessini basalts is reasonably below <100 °C. Similar conditions were also observed in the Deccan Traps in India (Greenberger et al., 2012), the Siletz River volcanics in Oregon (Keith and Staples, 1985), at Boron in California (Wise and Kleck, 1988) and in the Blackhead quarry in New Zealand (Graham et al., 2003).

According to the petrographic features and the chemical-mineralogical compositions, two different steps may be involved in the formation of the secondary mineral assemblages in the Lessini basalts: (1) earliest celadonite, silica and saponite crystallization (Stage I), followed by fine-grained, Ca- to Na-zeolites precipitation of the Stage II; (2) latest deposition of the larger crystals of the Ca-zeolites and calcite.

The earliest alteration step is related to post-magmatic mechanisms. The fractional crystallization of the hydrated, basaltic melt produces early formed anhydrous minerals during the cooling stage of the flow and a small amount of residual fluids with H_2O and volatiles. These residual and differentiated hot fluids may account for the first crystallization of clay minerals and zeolites (Stages I and II) in vesicular levels. All components necessary to form these mineral assemblages were readily available in the primary phases in the lavas. The deuteric alteration of the basalt flow has been proposed by various authors as a way to explain the occurrence of zeolites (e.g. Nasher and Davies, 1960; Wise and Kleck, 1988; Graham et al., 2003). In basaltic rocks with the restricted circulation of fluids, the composition of the glass, as well as the surrounding host rock, are the main factors controlling the composition of the zeolites (Wise, 1982). Conversely, because they typically have high fluid/rock ratios, there may be no control of fluid compositions by the host rocks in the hydrothermal systems. Studies of zeolite formation within basaltic rock sequences (e.g. Robert and Goffe, 1993; Neuhoff et al., 1997; Robert, 2001) highlight that zeolite crystallization occurred rapidly, both during and after volcanic activity, but prior to massive, medium-grade hydrothermal alteration. In the Lessini Mountains, the restriction of zeolite-bearing vesicles to the top of the basaltic sequences, and the crystallization of some zeolites directly upon fresh basalts, also attest to zeolite crystallization soon after lava emplacement and before significant hydrothermal alteration. The importance of the composition of the host rock as a controlling factor in the composition of the zeolites (Si/Al, as well as extra-framework cations) that occur in cavities of basalt has also been highlighted by a number of authors (e.g. Keith and Staples, 1985; Nasher and Davies, 1960; Wise, 1982; Bish and Ming, 2001).

In the second step, textural and compositional features of the latest mineral assemblages (Stage III) indicate a significant change in the crystallization conditions, perhaps related to the presence of new, possibly external, fluids which move within basaltic rocks during this later phase of alteration. As regards the source of these fluids, the geological data and tectonic relations with underlying calcareous marine sedimentary rocks in the Lessini Mountains (Piccoli, 1966; De Vecchi et al., 1976; Barbieri et al., 1982; 1991; De Vecchi and Sedea, 1995) suggest that locally heated surface water seems to be a likely source.

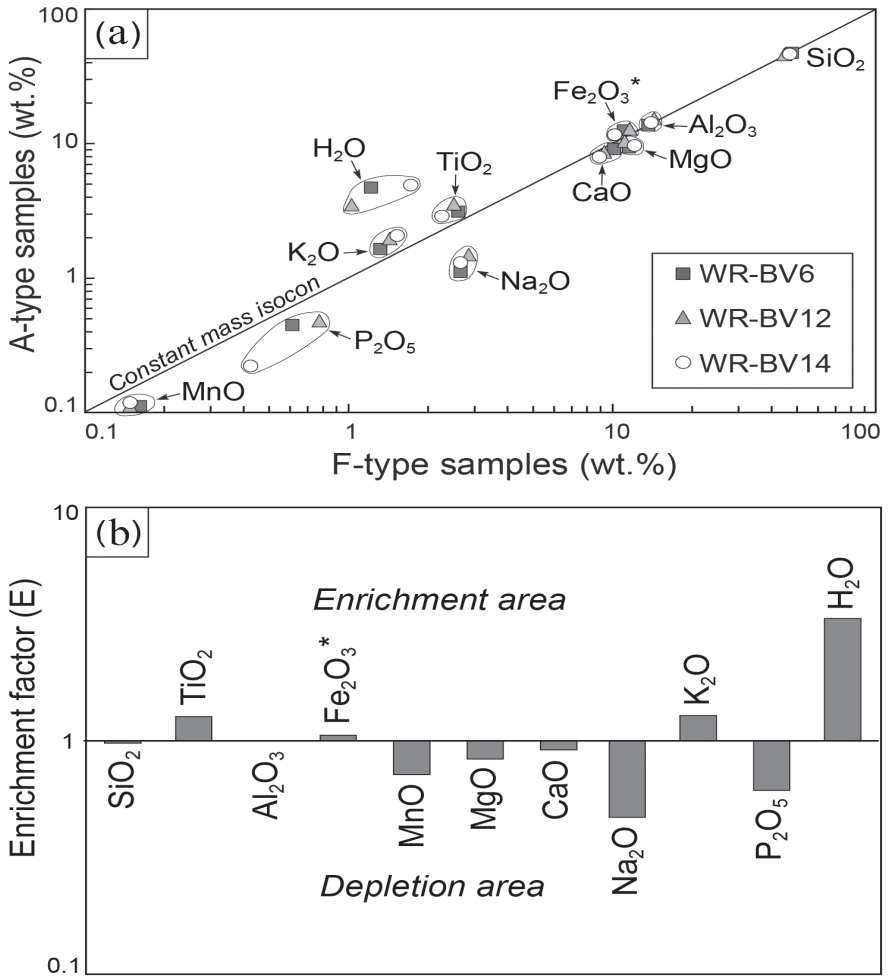

Figure 10. (a) Isocon plots (Grant, 1986) depicting the variation in bulk rock chemistry accompanying multistage alteration in the Lessini basalts. The lines labeled "constant mass isocon" depict the theoretical distribution of data assuming that the mass and compositions of the lavas do not change during alteration. (b) Bar chart showing average enrichment factors of the A-types with respect the F-Types. Values <1 indicate depletion and vice versa. Fe_2O_3*=total iron as Fe_2O_3.

The restricted distribution of coarse-grained zeolites in the Lessini basalts seems to support a genesis from localized fluids and/or heat, whereas there is no evidence of massive, medium-grade hydrothermal activity, such as deep wall-rock alteration and/or the crystallization of typical hydrothermal minerals (e.g. albite, actinolite, biotite, chlorite, chalcedony, and epidote). However, the presence of another juvenile hydrothermal component penetrating the entire volcanic sequence of the Lessini Mountains cannot be excluded. In this latest step, the Ca-dominate compositions of the zeolites might suggest that the zeolite-forming fluids may have interacted with the underlying calcareous marine sedimentary rocks through which the basalts erupted. The heat from these volcanic centres may have driven fluids through the sedimentary and volcanic pile, leaching Ca out of the calcareous sedimentary rocks. Furthermore, with a likely high concentration of carbonate ions in solution, the growth rate of zeolites would substantially increase due to the increased dissolution of silica from the surrounding rocks (Hawkins, 1981). This may also explain the common association of calcite with the Stage III Ca-rich zeolites in the Lessini basalts. Nonetheless, the overall abundance of calcite throughout the entire sequence of basaltic rocks from the Lessini Mountains seems to suggest that Ca was being continuously supplied to the zeolite-forming solutions.

The proposed multiphase alteration model is able to account for the major features observed and, even if it does not account for some points and neglets some geochemical and kinetic aspects, it provides at least a general framework for interpreting secondary mineralizations in basaltic rocks in low-T and Earth's surface conditions.

CONCLUDING REMARKS

The secondary mineral assemblages observed in the Tertiary basalts from the Lessini Mountains are dominated by clay minerals and zeolites and result from multistage alteration processes. The mineralogical, geochemical and textural signatures can be interpreted by three paragenetic stages, which can be related to the magmatic and thermal history of the lavas in the studied area. The earliest Stage I is characterized by the precipitation of clay and silica minerals along the inner walls of the vesicles. Stage II mineralization immediately following the Stage I products, and is characterized by the precipitation of fine-grained zeolites (erionite, offretite, analcime, natrolite, heulandite and stilbite). The final Stage III is marked by a new generation of coarse-grained, well-shaped zeolites (phillipstite-harmotomo, gmelinite, chabazite, willhendersonite and yugawaralite), followed by calcite.

The earliest alteration stages (I and II) could be related to post-magmatic mechanisms, and the elements necessary for secondary mineral formation derived from dissolution and hydrolysis of the primary igneous minerals and the volcanic glass of the host rock. Conversely, textural and compositional features of the final mineral assemblages (Stage III) seem to suggest a significant change in the crystallization conditions, probably related to the presence of new, perhaps external, late-stage fluids enriched in Ca and $(CO_3)^{2-}$. The chemical composition and mineralogy of the volcanic host rocks clearly control the formation of clay minerals and zeolites of the stages I and II. However, the composition of the underlying calcareous marine sedimentary rocks through which the volcanics erupted seems to play an important role in the zeolite formation of the final Stage III.

ACKNOWLEDGEMENTS

We would like to express our sincere thanks to Amleto Longhi (AMGV) for giving us the idea of studying secondary minerals in the Lessini basalt. We are also grateful to Franco Bressan, Dino Righetti and Guglielmino Salvatore for their help in the field and for providing us with high quality mineral specimens from their collections. Special thanks go to E. Salvioli Mariani (University of Parma) and L. Valentini (University of Urbino) for their assistance on the SEM observations and EDS analyses. Very useful comments by anonymous reviewers were greatly appreciated. We warmly thanks M. Lustrino and A. Gianfagna for their patience and editorial handling of the paper. Thanks are also due to Antoine van Maarle, for his help in revising the English style.

REFERENCES

Akizuki M. and Konno H. (1987) Growth twinning in phacolite. Mineralogical Magazine 51, 427-430.

Akizuki M., Nishido H., Fujimoto M. (1989) Herschelite: morphology and growth sector. The American Mineralogist 74, 1337-1342.

Alt J.C., Honnorez J., Laverne C., Emmermann R. (1986) Alteration of a 1 km section through the upper oceanic crust, DSDP Hole 504B: the mineralogy, chemistry and evolution of basalt-seawater interactions. Journal of Geophysical Researches 91, 10309-10335.

Andrada de Palomera P., van Ruitenbeek F.J.A., van der Meer F.K., Fernández R. (2012) Geochemical indicators of gold-rich zones in the La Josefina epithermal deposit, Deseado Massif, Argentina. Ore Geology Reviews 45, 61-80.

Armbruster Th., Wenger M., Kohler Th. (1991) Mischkristalle von Klinoptilolith-Heulandit und armotom-Phillipsit aus dem Basalt von Weitendorf, Steiermark. Mitteilungen der Abteilung fur Mineralogie des Landesmuseum 59, 13-18.

Barbieri G., De Zanche V., Sedea R. (1991) Vulcanesimo paleogenico ed evoluzione del semigraben Alpone-Agno (Monti Lessini). Rendiconti Società Geologica Italiana 14, 5-12.

Barbieri G., De Zanche V., Medizza F., Sedea R. (1982) Considerazioni sul vulcanismo terziario del Veneto occidentale e del Trentino meridionale. Rendiconti Società Geologica Italiana 4, 267-270.

Barth-Wirsching U. and Höller H. (1989) Experimental studies on zeolite formation conditions. European Journal of Mineralogy 1, 489-506.

Beccaluva L., Bianchini G., Bonadiman C., Coltorti M., Milani L., Salvini L., Siena F., Tassinari R. (2007) Intraplate litospheric and sublitospheric components in the Adriatic domain: nephelinite to tholeiite magma generation in the Paleogene Veneto volcanic province, southern Alps. Mineralogical Society of America, Special Paper 418, 131-152.

Beccaluva L., Bonadiman C., Coltorti M., Salvini L., Siena F. (2001) Depletion events, nature of metasomatizing agent and timing of enrichment processes in lithospheric mantle xenoliths from the Veneto Volcanic Province. Journal of Petrology 42, 173-187.

Bettison L.A. and Schiffman P. (1988) Compositional and structural variations of phyllosilicates from the Point Sal ophiolite, California. American Mineralogist 73, 62-76.

Bettison-Varga L., Mackinnon I.D., Schiffman P. (1991) Integrated TEM-XRD and electron microprobe investigation of mixed-layer chlorite-smectite from the Point Sal ophiolite, California. Journal of Metamorphic Geology 9, 697-710.

Birch W.D. (1988) Zeolites from Phillip Island and Flinders, Victoria. Mineralogical Record 19, 451-460.

Birch W.D. (1989) Chemistry of Victorian zeolites: Zeolites of Victoria. The Mineralogical Society of Victoria special publication 2, 91-102.

Bish D.L. and Ming D.W. (2001) Natural Zeolites: Occurrence, Properties, Applications. Mineralogical Society of America. Reviews in Mineralogy and Geochemistry 45, 662 pp.

Bonadiman C., Coltorti M., Milani L., Salvini L., Siena F., Tassinari R. (2001) Metasomatism in the lithospheric mantle and its relationships to magmatism in the Veneto Volcanic Province, Italy. Periodico di Mineralogia 70, 333-357.

Buckley H.A., Bevan J.C., Brown K.M., Johnson L.R. (1978) Glauconite and celadonite: two separate mineral species. Mineralogical Magazine 42, 373-82.

Cenni M. (2009) Le mineralizzazioni secondarie nelle rocce basaltiche: esempi dai Monti Lessini (Italia). PhD thesis, University of Urbino 'Carlo Bo', Italy, 193 pp.

Cerny P., Rinaldi R., Surdam R.C. (1977) Wellsite and its status in the phillipsite-harmotome group. Neues Jahrbuch für Mineralogie, Abhandlungen, 128, 312-330.

Coombs D.S., Alberti A., Armbruster T., Artioli G., Colella C., Galli E., Grice J.D., Liebau F., Mandarino J.A., Minato H., Nickel E.H., Passaglia E., Peacor D.R., Quartieri S., Rinaldi R., Ross M., Sheppard R.A., Tillmans E., Vezzalini G. (1998) Recommended nomenclature for zeolite minerals: report of the subcommittee on zeolites of the International Mineralogical Association, Commission on New Minerals and Mineral Names. Mineralogical Magazine 62, 533-571.

Coombs D.S., Ellis A.J., Fyfe W.S., Taylor A.M. (1959) The zeolite facies, with comments on the interpretation of hydrothermal syntheses. Geochemical and Cosmochemical Acta 17, 53-107.

De Vecchi G.P., Gregnanin A., Piccirillo E.M. (1976) Aspetti petrogenetici del vulcanesimo terziario veneto. Memorie Istituto di Geologia e Mineralogia dell'Universita di Padova 30, 1-32.

De Vecchi G.P. and Sedea R. (1995) The Paleogene basalt of the Veneto region (NE Italy). Memorie Istituto di Geologia e Mineralogia dell'Università di Padova 47, 253-274.

Deer W.A., Howie R., Wis W.S., Zussman J. (2004) Rock Forming Minerals. Framework Silicates: Silica Minerals, Feldspathoids and the Zeolites. The Geological Society London 4B, second editions, 982 pp.

Degraff J.M., Long P.E., Aydin A. (1989) Use of joint-growth directions and rock textures to infer thermal regimes during solidification of basaltic lava flows. Journal of Volcanology and Geothermal Research 38, 309-324.

Eberlein G.D., Erd R.C., Weber F., Beatty L.B. (1971) New occurrence of yugawaralite from the Chena Hot Springs area, Alaska. The American Mineralogist 56, 1699-1717.

Eggleton R.A. and Keller J. (1982) The palagonitization of limburgite glass - a TEM study. Neues Jahrbuch Mineral Monatsh 321-336.

Franzson H., Zierenberg R., Schiffman P. (2008) Chemical Transport in Geothermal Systems in Iceland. Evidence from Hydrothermal Alteration. Journal of Volcanology and Geothermal Research 173, 217-229.

Galli E. (1972) La phillipsite barifera ("wellsite") di M. Calvarina (Verona). Periodico di Mineralogia 41, 23-33.

Ghiara M.R., Franco E., Petti C., Stanzione D., Valentino G.M. (1993) Hydrothermal interaction between basaltic glass, deionized water and seawater. Chemical Geology 104, 125-138.

Gianelli G., Mekuria N., Battaglia S., Chersicla A., Garofano P., Ruggeri G., Manganelli M., Gebregziabher Z. (1998) Water-rock interaction and hydrothermal mineral equilibria in the Tendaho geothermal system. Journal of Volcanology and Geothermal Research 86, 253-276.

Gíslason S.R. and Eugster H. (1987) Meteoric water-basalt interaction: I. A laboratory study. Geochimica et Cosmochimica Acta 51, 2827-2840.

Graham I.T., Pogson R.E., Colchester D.M., Baines A. (2003) Zeolite crystal habits, compositions, and paragenesis, Blackhead Quarry, Dunedin, New Zealand. Mineralogical Magazine 67, 625-637.

Grant J.A. (1986) The Isocon Diagram A Simple Solution to Gresens' Equation for Metasomatic Alteration. Economic Geology 81, 1976-1982.

Greenberger R.N., Mustard J.F., Kumar P.S., Dyar M.D., Breves E.A., Sklute E.C. (2012) Low temperature aqueous alteration of basalt: Mineral assemblages of Deccan basalts and implications for Mars. Journal of Geophysical Research 117, doi:10.1029/2012JE004127.

Gysi A.P. and Stefánsson A. (2012) CO_2-water-basalt interaction. Low temperature experiments and implications for CO_2 sequestration into basalts. Geochimica et Cosmochimica Acta 81, 129-152.

Hansen S. (1990) Harmotome from Odarslov, Skaane, Sweden. Geologiska Foreningens I Stockolm Forhandlingar 112, 140.

Hawkins D.B. (1981) Kinetics of glass dissolution and zeolite formation under hydrothermal conditions. Clays and Clay Minerals 29, 331-340.

Hay R.L. (1970) Silicate reactions in three lithofacies of a semi-arid basin, Olduvai Gorge, Tanzania. Mineralogical Society of America, Special Paper 3, 237-255.

Höller H. and Wirsching U. (1988) Experiments on the formation conditions and morphology of chabazite from volcanic glasses. In: Occurrence, Proprieties, and Utilization of Natural Zeolites. (eds.): D. Kalló and H.S. Sherry, Akadémiai Kiadó, Budapest 171-191.

Jiang S.Y., Wang R.C., Xu X.S., Zhao K.D. (2005) Mobility of high field strength elements (HFSE) in magmatic-, metamorphic-, and submarine-hydrothermal systems. Physics and Chemistry of Earth 30, 1020-1029.

Karrat L., Perruchot A. and Macaire J.-J. (1998) Weathering of a Quaternary glass-rich basalt in Bakrit, Middle Atlas Mountains, Morocco. Comparison with a glass-poor basalt. Geodinamica Acta 11, 205-215.

Keith T.E.C. and Staples L.W. (1985) Zeolites in Eocene basaltic pillow lavas of the Siletz River Volcanics, central Coast Range, Oregon. Clays and Clay Minerals 33, 135-144.

Kousehlar M., Weisenberger T., Tutti F., Mirnejad H. (2012) Fluid control on low-temperature mineral formation in volcanic rocks of Kahrizak, Iran. Geofluids 12, 295-311.

Kristmannsdottir H. and Tomasson J. (1978) Zeolites zones in geothermal areas of Iceland. In: Natural Zeolite Occurrence, Properties and Use. (eds.): L.B. Sand and F.M. Mumpton, Pergamon Press, Oxford, UK, 277-284.

Luppi D., Carbonin S., Boscardin M., Pegoraro S. (2007) Chabazite e gmelinite del Vicentino: distribuzione e cristallochimica. Rivista Mineralogica Italiana 1, 8-21.

Marescotti P., Vanko D.A., Cabella R. (2000) From oxidizing to reducing alteration: mineralogical variations in pillow basalts from the East Flank, Juan de Fuca Ridge. Proceedings of the Ocean Drilling Program, Scientific Results 168, 119-136.

Markússon S.H. and Stefánsson A. (2011). Geothermal surface alteration of basalts, Krýsuvk Iceland - alteration mineralogy, water chemistry and the effects of acid supply on the alteration process. Journal of Volcanology and Geothermal Research 206, 46-59.

Mas A., Guisseau D., Patrier Mas P., Beaufort D., Genter A., Sanjuan B., Girard J.P. (2006) Clay minerals related to the hydrothermal activity of the Bouillante geothermal field (Guadeloupe). Journal of Volcanology and Geothermal Research 158, 380-400.

Mattioli M., Cenni M., Raffaelli G. (2008) I minerali del veronese: le mineralizzazioni secondarie delle rocce vulcaniche dei Monti Lessini. Memorie del Museo civico di storia naturale di Verona. Sezione Scienze della terra 7, 196 pp.

Mattioli M., Menichetti M., Renzulli A., Toscani L., Salvioli-Mariani E., Suarez P., Murroni A. (2014) Genesis of the hydrothermal gold deposits in the Canan area, Lepaguare District, Honduras. International Journal of Earth Sciences 103, 901-928.

McMillan K., Cross R.W., Long P.E. (1987) Two-stage vesiculation in the Cohassett flow of the Grande Ronde Basalt, south-central Washington. Geology 15, 809-812.

Mees F., Stoops G., Van Ranst E., Paepe R., Van Overloop E. (2005) The nature of zeolite occurrences in deposits of the Olduvai basin, northern Tanzania. Clays and Clay Minerals 53, 659-673.

Milani L., Beccaluva L., Coltorti M. (1999) Petrogenesis and evolution of the Euganean magmatic complex, Veneto Region, North-East Italy. European Journal of Mineralogy 11, 379-399.

Mottl M.J. (1983) Metabasalts, axial hot springs, and structure of hydrothermal systems at mid-ocean ridges. Geological Society of America Bulletin 94, 161-180.

Nakamura K., Kato Y., Tamaki K., Ishii T. (2007) Geochemistry of hydrothermally altered basaltic rocks from the Southwest Indian Ridge near the Rodriguez Triple Junction. Marine Geology 239, 125-141.

Nashar B. and Basden R. (1965) Solubility of basalt under atmospheric conditions of temperature and pressure. Mineralogical Magazine 35, 408-411.

Nashar B. and Davies M. (1960) Secondary minerals of the Tertiary basalts, Barrington, New South Wales. Mineralogical Magazine 32, 480-411.

Neuhoff P.S., Fridriksson T., Anorsson S., Bird D.K. (1999) Porosity evolution and minerals paragenesis during low-grade metamorphism of basaltic lavas at Teigarhorn, eastern Iceland. American Journal of Science 299, 467-501.

Neuhoff P.S., Fridriksson T., Bird D.K. (2000) Zeolite paragenesis in the north atlantic igneous province: implications for geotectonics and groundwater quality of basaltic crust. International Geology Reviews 42, 15-44.

Neuhoff P.S., Rogers K.L., Stannius L.S., Bird D.K., Pedersen A.K. (2006) Regional very low-grade metamorphism of basaltic lavas, Disko-Nuussuaq region, West Greenland. Lithos 92, 33-54.

Neuhoff P.S., Watt W.S., Bird D.K., Pedersen A.K. (1997) Timing and structural relations of regional zeolite zones in basalts of the East Greenland continental margin. Geology 25, 803-806.

Papazzoni C. and Trevisani E. (2006) Facies analysis, palaeoenvironmental reconstruction, and biostratigraphy of the "Pesciara di Bolca" (Verona, northern Italy): an early Eocene Fossil-Lagerstätte. Palaeogeography, Palaeoclimatology, Palaeoecology 242, 21-35.

Passaglia E. (1970) The crystal chemistry of chabazites. The American Mineralogist 55, 1278-1301.

Passaglia E., Artioli G., Gualtieri A. (1998) Crystal chemistry of the zeolites erionite and offretite. The American Mineralogist 83, 577-589.

Passaglia E. and Bertoldi G. (1983) Harmotome from Selva di Trissino (Vicenza, Italy). Periodico di Mineralogia 52, 75-82.

Passaglia E., Pongiluppi D., Vezzalini G. (1978) The crystal chemistry of gmelinites. Neues Jahrbuch Für Mineralogie Monatshefte 310-324.

Passaglia E. and Sheppard R.A. (2001) The Crystal Chemistry of Zeolites. In: Reviews in Mineralogy and Geochemistry. (eds.): D.L. Bish and. D.W. Ming 45, 69-116.

Passaglia E., Tagliavini A., Gutoni R. (1996) Offretite and other zeolites from Fittà (Verona, Italy). Neues Jahrbuch Für Mineralogie Monatshefte 418-428.

Piccoli G. (1966) Studio geologico del vulcanismo paleogenico veneto. Memorie Istituto di Geologia e Mineralogia dell'Università di Padova 26, 100 pp.

Pongiluppi D. (1977) A new occurence of yugawaralite at Osilo, Sardinia. The Canadian Mineralogist 15, 113-114.

Robert C. (1988) Barian phillipsite and strontian chabazite from the Plateau des Coirons, Ardeche, France. Bulletin de Minéralogie 111, 671-677.

Robert C. (2001) Hydrothermal alteration processes of the Tertiary lavas of Northern Ireland. Mineralogical Magazine 65, 543-554.

Robert C. and Goffé B. (1993) Zeolitization of basalts in suacqueous freshwater settings: field observations and experimental study. Geochimica Cosmochimica Acta 57, 3597-3612.

Robert C., Goffe B., Saliot P. (1988) Zeolitization of a basaltic flow in a continental environment; an example of mass transfer under thermal control. Bulletin de Minéralogie 111, 207-223.

Robinson D., Bevins R.E., Rowbotham G. (1993) The characterization of mafic phyllosilicates in low-grade metabasalts from eastern North Greenland. American Mineralogist 78, 377-390.

Rogers K., Neuhoff P., Pedersen A., Bird D. (2006) CO_2 metasomatism in a basalt hosted petroleum reservoir, Nuussuaq, West-Greenland. Lithos 92, 55-85.

Schenato F. Formoso, M.L.L., Dudoignon P., Meunier A., Proust D., Mas A. (2003) Alteration processes of a thick basaltic lava flow of the Paranà Basin (Brazil): petrographic and mineralogical studies. Journal of South American Earth Sciences 16, 423-444.

Schiffman P. and Fridleifsson G.O. (1991) The smectite-chlorite transition in drillhole NJ-15, Nesjavellir geothermal field, Iceland: XRD, BSE and electron microprobe investigations. Journal of Metamorphic Geology 9, 679-696.

Senderov E.E. (1989) Physical-chemical aspects on zeolite formation in nature. In: Occurrence, Properties and Utilization of Natural Zeolites. (eds): D. Kallò and H.S. Sherry, Akademiai Kiado, Budapest, Hungary, 111-147.

Seyfried W.E. and Bischoff J.L. (1979) Low temperature basalt alteration by seawater: An experimental study at 70 °C and 150 °C. Geochimica et Cosmochimica Acta 43, 1937-1947.

Talbi E.H. and Honnorez J. (2003) Low-temperature alteration of Mesozoic oceanic crust, Ocean Drilling Program Leg 185. Geochemistry Geophysic Geosystem 4, 8906. doi:10.1029/2002GC000405.

Teagle D.A.H., Alt J.C., Bach W., Halliday A.N., Erzinger J. (1996) Alteration of upper oceanic crust in a ridge-flank hydrothermal upflow zone: mineral, chemical, and isotopic constraints from Hole 896A. Proceedings ODP Scientific Results 148, 119-150.

Tschernich R.W. and Wise W.S. (1982) Paulingite: variations in composition. American Mineralogist 67, 799-803.

Tuchschmid M.P. (1992) Petrogenese der anorogenen Tertiären vulkanite der venezianischen vulkanprovinz (N-Italien). Theses. Inst. Mineral. Petrogr. Zurig, ETH Zurig, 207 pp.

Ueda S., Nishimura M., Koizumi M. (1985) Synthesis of offretite-erionite type zeolite from solution phase. In: Zeolites, synthesis, structure, technology and application. (eds.): B. Držaj, S. Hocevar and S. Pejovnick, Elsevier, Amsterdam, 105-110.

Verma S.P. (1981) Sea water alteration effects on $^{87}Sr/^{86}Sr$, K, Rb, Cs, Ba, and Sr in oceanic igneous rocks. Chemical Geology 34, 81-89.

Verma S.P. (1992) Seawater alteration effects on REE, K, Rb, Cs, Sr, U, Th, Pb and Sr-Nd-Pb isotope systematics in Mid-Ocean Ridge Basalt. Geochemical Journal 26, 159-177.

Vezzalini G., Quartieri S., Galli E. (1997) Occurrence and crystal

structure of a Ca-pure willhendersonite. Zeolites 19, 75-79.
Vezzalini G., Quartieri S., Rossi A., Alberti A. (1994) Occurrence of zeolites from northern Victoria Land (Antarctica). Terra Antarctica 1, 96-99.
Walker G.P.L. (1960a) Zeolite zones and dyke distribution in relation to the structure of the basalts of eastern Iceland. The Journal of Geology 68, 515-528.
Walker G.P.L. (1960b) The amygdale minerals of the Tertiary lavas of Ireland. III. Regional distribution. Mineralogical Magazine 32, 515-528.
Weisenberger T. and Bucher K. (2011) Mass transfer and porosity evolution during low temperature water-rock interaction in gneisses of the Simano nappe: Arvigo, Val Calanca, Swiss Alps. Contributions to Mineralogy and Petrology 162, 61-81.
Weisenberger T. and Selbekk R.S. (2009) Multi-stage zeolite facies mineralization in the Hvalfjördur area, Iceland. International Journal of Earth Sciences 98, 985-999.
Weisenberger T. and Spürgin S. (2009) Zeolites in alkaline rocks of the Kaiserstuhl volcanic complex, SW Germany - new micropobe investigation and their relationship to the host rock. Geologica Belgica 12, 75-91.
Weisenberger T.B., Spürgin S., Lahaye Y. (2014) Hydrothermal alteration of the Fohberg phonolite, Kaiserstuhl Volcanic Complex, Germany. International Journal of Earth Sciences 103, 2273-2300.
Winchester J.A. and Floyd P.A. (1976) Geochemical magma type discrimination; application to altered and metamorphosed basic igneous rocks. Earth and Planetary Science Letters 28, 459-469.
Wise W.S. (1982) New occurrence of faujasite in southeastern California. American Mineralogy 67, 794-798.
Wise W.S. and Kleck W.D. (1988) Sodic clay-zeolite assemblage in basalt at Boron, California. Clays and Clay Minerals 36, 131-136.
Zampieri D. (1995) Tertiary extension in the southern Trento Platform, Southern Alps, Italy. Tectonics 14, 645-657.
Zampieri D. (2000) Segmentation and linkage of the Lessini Mountains normal Faults, Southern Alps, Italy. Tectonophysics 319, 19-31.
Zeng Y. and Liou J.G. (1982) Experimental investigation of yugawaralite-wairakite equilibrium. American Mineralogist 67, 937-943.